CDS Technical Report 94-014
California Institute of Technology
Submitted to J. Robotic Systems, Sep 94

GEOMETRIC PHASES AND ROBOTIC LOCOMOTION

SCOTT D. KELLY AND RICHARD M. MURRAY

Division of Engineering and Applied Science
California Institute of Technology
Pasadena, California 91125

September 6, 1994

ABSTRACT. Robotic locomotion is based in a variety of instances upon cyclic changes in the shape of a robot mechanism. Certain variations in shape exploit the constrained nature of a robot's interaction with its environment to generate net motion. This is true for legged robots, snakelike robots, and wheeled mobile robots undertaking maneuvers such as parallel parking. In this paper we explore the use of tools from differential geometry to model and analyze this class of locomotion mechanisms in a unified way. In particular, we describe locomotion in terms of the geometric phase associated with a connection on a principal bundle, and address issues such as controllability and choice of gait. We also provide an introduction to the basic mathematical concepts which we require and apply the theory to numerous example systems.

1. INTRODUCTION

The term "locomotion" refers to autonomous movement from place to place. Robotic locomotion employs a variety of mechanisms. Though most of today's mobile robots have wheels or legs, other classes of robots—such as hyper-redundant, snakelike robots—are becoming increasingly popular. Traditionally, distinct methods of locomotion have been studied separately, and most approaches have relied on the specific properties of a given system to analyze its locomotive capabilities.

Despite their differences in approach, however, most robotic locomotion systems share certain common features. Many involve motion in either two or three dimensional Euclidean space. Land based robots almost always rely upon interaction with the environment to achieve motion. These robots push, slide, and roll along the ground. A variety of systems, furthermore, rely on periodic control inputs to achieve motion in certain directions.

The use of periodic inputs to generate motion is particularly intriguing since it is the *rectification* of these inputs which characterizes locomotion. By changing the basic shape of a robot in a cyclic fashion, net motion in some direction can be

achieved. A good example of this is parallel parking a car: by cycling the steering wheel and driving back and forth in proper phase, it is possible to realize a net sideways motion of the car. In fact, using a simple model for the kinematics of an automobile, it can be shown that driving back and forth once while turning the steering wheel back and forth twice with the same period results in a net sideways motion.

Similar descriptions apply to many other systems. Snakes undergo cyclic changes in shape to achieve net motion. Legged locomotion is characterized by the proper phasing of repetitive leg movements. Indeed, even driving a car in a straight line can be viewed as periodic motion of the wheels of the car, using the natural equivalence of the angles of rotation 2π and 0.

This use of cyclic motion is characteristic of the concept of *geometric phases* in geometric mechanics. In studying the motion of a satellite controlled using momentum wheels, for example, the net rotation of the satellite due to a periodic motion of the wheels can be determined by analyzing the conservation law for angular momentum. The geometric phase associated with the motion of the rotors is a measure of this rotation. (See Marsden et al. [15] for a detailed description of the role of geometric phases in mechanics.)

In this paper, we explore the use of geometric phases to study locomotion for a variety of systems. This paper is a modest attempt to provide a framework for understanding locomotion by concentrating on geometric structure. Indeed, this theory is as yet quite incomplete, and requires further justification and revision of the problem formulation. We hope that by posing problems in this way, we can begin to build a comprehensive theory for locomotion which is at once mathematically rigorous, elegant, and enlightening.

Locomotion has long intrigued the human mind. Since "the way of an eagle in the air [and] the way of a serpent upon a rock" perplexed the author of Proverbs 30:19, man has struggled for a clear understanding of the locomotive principles he has observed. Centuries ago, Leonardo da Vinci applied his knowldege of anatomy to a pictorial study of the human form in motion, presaging the landmark photographic studies of Eadweard Muybridge collected in [22] and [23]. According to Sir James Gray [6], however, advancements in the quantitative description of animal locomotion were few until the present; Gray cites Borelli's (17th century) *De motu animalium* and Marey's *Machine Animale* (1873) as rare works of significance.

Since the invention of the wheel, we as engineers have sought to devise artificial means for locomotion. Indeed, the wheel's role in the history of man-made locomotion systems cannot be overestimated. Variable geometry wheeled and tracked vehicles, such as military tanks, have overcome many of the traditional difficulties of wheeled vehicles on rough terrain.

Within the last century, however, we have been able to look beyond the wheel to better emulate nature in our designs. As early as 1940, A. C. Hutchinson and F. S. Smith [10] built a small robot which was able to walk and ascend obstacles on four independently-controlled legs. The General Electric Walking Truck, designed and built in the 1960s, epitomizes large legged vehicles under strictly mechanical

control [19]. The last two decades have witnessed the construction of several walking robots with two to six legs, as well as M. H. Raibert's hopping machines with as few legs as one [25], [24]. R. Tomovic and W. J. Karplus [28] first applied mathematical methods, including the theory of finite states, to the analysis of legged locomotion. Hildebrand [7] and McGhee [17] formalized the analysis of walking gaits. Recent research into the dynamics and control of legged machines has included McGeer's work on passive dynamic walking [16].

S. Hirose and Y. Umetani began their work with snakelike hyper-redundant robots, or "active cord mechanisms," in the 1970s. An early creation of theirs [8] propelled itself in a snakelike fashion but was itself confined to the plane; a later robot [9] could lift sections of its body for maneuvers which included climbing stairs. The kinematics of hyper-redundant robot locomotion have been analyzed more recently by Chirikjian and Burdick, for example in [5].

Perhaps the earliest geometric approach to a problem in locomotion was that of Shapere and Wilczek [27], who studied locomotion in fluids at very low Reynolds number using techniques from gauge theory. They showed that the motion of paramecia could be understood by calculating the geometric phase with respect to a certain connection on a principal fiber bundle (these terms will all be defined shortly). The connection, which described how changes in shape affected the position of a paramecium, was determined by the underlying fluid dynamics.

The use of geometric phases and holonomy to understand locomotion has also appeared in the mobile robotics literature. In [21], Murray and Sastry demonstrated the rectification of sinusoidal motions in a broad class of systems, including a kinematic model of a car. As we shall see in the sequel, the nonholonomic constraints which describe the pure rolling condition on the wheels of a car can be modeled using a connection on a principal bundle, and the geometric phase associated with motion of the car's inputs describes the net motion of the car.

As these examples illustrate, locomotion often relies on periodic variations in a system's internal (or shape) variables. In the remainder of this paper, we explore the mathematics needed to study the geometry of these and other locomotion systems.

This paper is organized as follows. In Section 2 we provide an introduction to principal bundles and connections, specialized to the case of subgroups of the special Euclidean group $SE(3)$ acting trivially on open subsets of $\mathbb{R}^m$. This case corresponds to exactly what we need to study the relationship between locomotion and geometric phases. Section 3 describes this relationship in detail for several classes of examples. In particular, we describe how the constraints on the interaction of a robot with its environment can be modeled as a connection on a principal bundle and how geometric phases can be used to represent locomotion. Section 4 concentrates on controllability properties of the resulting systems and includes some new characterizations of controllability on principal bundles. An extended set of examples is provided in Section 5, and a summary of our results and a discussion of future work are given in Section 6.

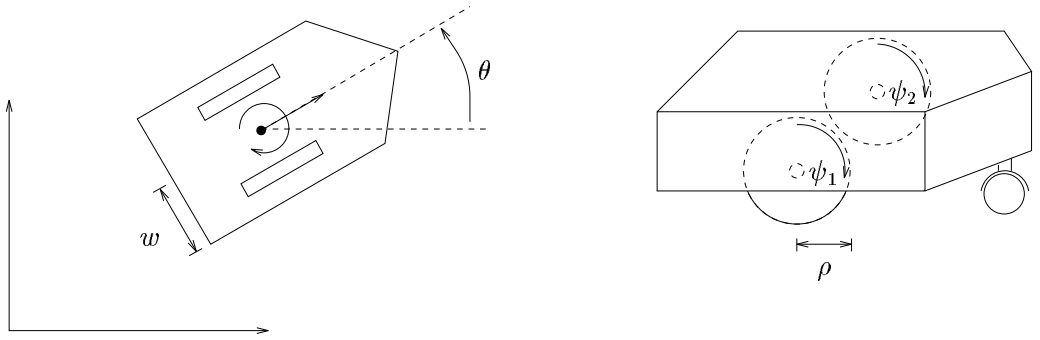

FIGURE 1. Two wheeled planar mobile robot.

2. Mathematical Preliminaries

In this section we describe some mathematical tools which will be used in the sequel. We restrict our treatment to certain special cases of the general theory when appropriate. Our emphasis is on providing formulas which can be used for computation on subsequent problems. References to more complete treatments of the underlying mathematics are given in each subsection. We begin with an example to illustrate the role of the mathematics we describe.

2.1. Example. Consider the dynamics of a two wheeled mobile robot which is able to drive in the direction in which it points and spin about its center, as shown in Figure 1. Let ψ_1 and ψ_2 denote the angle of a fixed point on each wheel with respect to the vertical. The position of the robot is given by the xy location of its center and the heading angle θ. Balance is maintained by a small castor whose effect we shall ignore. Thus $q = (\psi_1, \psi_2, x, y, \theta)$ denotes the configuration of the system.

The motion of the system is governed by Lagrange's equations, taking into account the constraints which describe the contact of the wheels with the ground. We model each contact using a *pure rolling* assumption: each wheel can roll in the direction in which it points and spin about its vertical axis, but cannot slide perpendicular to its rolling direction. A simple calculation shows that the assumption of pure rolling yields constraints

$$\begin{aligned} \omega^1(q)\dot{q} &= \dot{x}\cos\theta + \dot{y}\sin\theta - \frac{\rho}{2}(\dot{\psi}_1 + \dot{\psi}_2) = 0 \\ \omega^2(q)\dot{q} &= -\dot{x}\sin\theta + \dot{y}\cos\theta = 0 \\ \omega^3(q)\dot{q} &= \dot{\theta} - \frac{\rho}{2w}(\dot{\psi}_1 - \dot{\psi}_2) = 0. \end{aligned} \tag{1}$$

Linear velocity constraints such as these are called *Pfaffian constraints.*

The Lagrangian for the system is given by

$$L(q,\dot{q}) = \frac{1}{2}m(\dot{x}^2 + \dot{y}^2) + \frac{1}{2}J\dot{\theta}^2 + \frac{1}{2}J_2(\dot{\psi}_1^2 + \dot{\psi}_2^2),$$

where m is the mass of the robot, J its inertia, and J_w the inertia of the wheels. (We have assumed for simplicity's sake that the center of mass of the robot lies on

the line between the two drive wheels.) Using Lagrange multipliers, the dynamics of the system can be shown to satisfy

$$\begin{bmatrix} \frac{m\rho^2}{4} + \frac{J\rho^2}{4w^2} + J_2 & \frac{m\rho^2}{4} - \frac{J\rho^2}{4w^2} \\ \frac{m\rho^2}{4} - \frac{J\rho^2}{4w^2} & \frac{m\rho^2}{4} - \frac{J\rho^2}{4w^2} + J_w \end{bmatrix} \begin{bmatrix} \ddot{\psi}_1 \\ \ddot{\psi}_2 \end{bmatrix} = \begin{bmatrix} \tau_1 \\ \tau_2 \end{bmatrix} \tag{2}$$

$$\begin{aligned} \dot{x}\cos\theta + \dot{y}\sin\theta - \frac{\rho}{2}(\dot{\psi}_1 + \dot{\psi}_2) &= 0 \\ -\dot{x}\sin\theta + \dot{y}\cos\theta &= 0 \\ \dot{\theta} - \frac{\rho}{2w}(\dot{\psi}_1 - \dot{\psi}_2) &= 0, \end{aligned} \tag{3}$$

where τ_1 and τ_2 are the torques applied to the drive wheels. Notice that the last three equations are the constraints and that, given ψ_1 and ψ_2 as functions of time, we can uniquely solve for $\dot{x}$, $\dot{y}$, and $\dot{\theta}$.

This system has a number of features which are characteristic of locomotion systems in general. We split the configuration variables into two sets, calling (ψ_1, ψ_2) the *internal variables* and (x, y, θ) the *group variables*. The latter choice reflects the fact that planar position and orientation describe a subgroup of the group of rigid motions. The dynamics for the system consist of a set of second order equations which describe the motion of the internal variables and a set of first order equations which describe how the group variables evolve. We refer to the second order equations (2) as the *reduced dynamics*. Since our control inputs τ_1 and τ_2 enter directly into the reduced dynamics, we can follow any path in ψ_1 and ψ_2 by appropriate choice of input.

Given a trajectory in the internal variables, the constraint equations (3) can be solved for the corresponding motion in the group variables. This procedure is called *reconstruction*. Note that the torques required to follow a particular trajectory in the internal variables are not needed in the reconstruction process. Only the internal variables and their velocities appear in the constraint equations. In the remainder of this paper, we will focus on the reconstruction process and the modeling of a system's constraint kinematics.

We will always describe the position and orientation of a robot in terms of a subgroup of the special Euclidean group in $\mathbb{R}^3$. In this example we consider the subgroup of planar motion, $SE(2)$, but other subgroups will arise. Many features common to locomotion systems follow from general properties of rigid body motion. We now review some of these properties.

2.2. Rigid body motion. We give a brief introduction to rigid body motion in $\mathbb{R}^3$ for the purposes of establishing notation and presenting the formulas we will need. A more detailed description can be found in Murray et al. [20].

A rigid body consists of a set of points in $\mathbb{R}^3$ whose relative positions are fixed. The configuration of a rigid body is specified by attaching a coordinate frame to the body and describing its position and orientation relative to a fixed inertial frame.

We use the notation $g = (p, R)$ to denote the position and orientation of the body frame. The set of all such pairs is denoted $SE(3)$, the special Euclidean group on $\mathbb{R}^3$.

The group operation on $SE(3)$ is given by

$$g_1 \circ g_2 = (p_1 + R_1 p_2, R_1 R_2),$$

and describes the composition of two rigid body motions. It will often be convenient to use the homogeneous representation of $SE(3)$ in terms of 4×4 matrices, in which case the group operation becomes matrix multiplication, as follows:

$$g = \begin{bmatrix} R & p \\ 0 & 1 \end{bmatrix} \qquad g_1 g_2 = \begin{bmatrix} R_1 & p_1 \\ 0 & 1 \end{bmatrix} \begin{bmatrix} R_2 & p_2 \\ 0 & 1 \end{bmatrix}.$$

We will adopt the notation of homogeneous transformations and write $g_1 g_2$ for $g_1 \circ g_2$.

The velocity of a rigid body is described by a twist $\xi \in se(3)$. We use the *body velocity* defined in [20]:

$$\widehat{\xi} = g^{-1}\dot{g} = \begin{bmatrix} R^T\dot{R} & R^T p \\ 0 & 0 \end{bmatrix} = \begin{bmatrix} \widehat{\omega} & v \\ 0 & 0 \end{bmatrix}. \tag{4}$$

The skew-symmetric matrix $\widehat{\omega} \in \mathbb{R}^{3\times 3}$ represents the cross product of $\omega \in \mathbb{R}^3$ with another vector: $\widehat{\omega}a = \omega \times a$ for $a \in \mathbb{R}^3$. We call $\xi = (v, \omega) \in \mathbb{R}^6$ the twist coordinates of the velocity $\widehat{\xi} = g^{-1}\dot{g}$. Velocities are transformed between coordinate frames using the adjoint transformation $\mathrm{Ad}_g : se(3) \to se(3)$ given by $\mathrm{Ad}_g \widehat{\xi} = g\widehat{\xi}g^{-1}$. In twist coordinates this transformation is represented by the 6×6 matrix

$$\mathrm{Ad}_g = \begin{bmatrix} R & \widehat{p}R \\ 0 & R \end{bmatrix}. \tag{5}$$

We remark that the body velocity defined here is interpreted as the angular and translation velocity relative to the instantaneous body frame.

We will also make frequent use of the *Lie bracket* on $SE(3)$. Let $\xi_1, \xi_2 \in \mathbb{R}^6$ be two velocity vectors as defined above. Then the Lie bracket between ξ_1 and ξ_2 is given by

$$[\widehat{\xi}_1, \widehat{\xi}_2] = \widehat{\xi}_1\widehat{\xi}_2 - \widehat{\xi}_2\widehat{\xi}_1 \qquad \text{or} \qquad [\xi_1, \xi_2] = \begin{bmatrix} \omega_1 \times v_2 - \omega_2 \times v_1 \\ \omega_1 \times \omega_2 \end{bmatrix}, \tag{6}$$

where the second expression is given in twist coordinates. The Lie bracket is a measure of the commutativity between the rigid motions generated by moving with the velocities ξ_1 and ξ_2.

In this paper we will be primarily interested in several proper subgroups of $SE(3)$. The simplest subgroups will be pure translation along a line and pure translation in a plane. In either of these cases we represent the position of a rigid body as $p \in \mathbb{R}^k$, $k = 1, 2$, and the body velocity becomes $\xi = \dot{p}$. The Lie bracket for pure translational motion is always zero. This is easily verified by setting $R = I$ and $\omega = 0$ in the previous formulas.

One of the main subgroups of $SE(3)$ which appears in locomotion problems is $SE(2)$, the group of *planar rigid motions*. A point in $SE(2)$ can be written as

$$p = \begin{bmatrix} x \\ y \\ \theta \end{bmatrix} \qquad R = \begin{bmatrix} \cos\theta & -\sin\theta & 1 \\ \sin\theta & \cos\theta & 0 \\ 0 & 0 & 1 \end{bmatrix}. \tag{7}$$

For brevity we often will write $g = (x, y, \theta) \in SE(2)$ and the group operation becomes

$$g_1 \circ g_2 = \begin{bmatrix} x_1 + x_2\cos\theta_1 - y_2\sin\theta_1 \\ y_1 + x_2\sin\theta_1 + y_2\cos\theta_1 \\ \theta_1 + \theta_2 \end{bmatrix}. \tag{8}$$

The velocity of a rigid motion in $SE(2)$ is given by

$$\widehat{\xi} = g^{-1}\dot{g} \qquad \xi = \begin{bmatrix} v_x \\ v_y \\ \omega \end{bmatrix} = \begin{bmatrix} \dot{x}\cos\theta + \dot{y}\sin\theta \\ \dot{y}\cos\theta - \dot{x}\sin\theta \\ \dot{\theta} \end{bmatrix} \tag{9}$$

and the Lie bracket becomes

$$[\xi_1, \xi_2] = \begin{bmatrix} \omega_1 v_{2y} - \omega_2 v_{1y} \\ \omega_2 v_{1x} - \omega_1 v_{2x} \\ 0 \end{bmatrix}. \tag{10}$$

Other subgroups of $SE(3)$ are also possible. For "locomotion" problems involving satellites and other space-based systems, one is often interested in purely rotational motion. In this case we write $R \in SO(3)$ for the configuration and a velocity is written as $\widehat{\omega} \in so(3)$. The Lie bracket on $SO(3)$ is given by the cross product: $[\omega_1, \omega_2] = \omega_1 \times \omega_2$.

We also make use of the *exponential map*. The exponential map takes a velocity vector and returns the rigid motion corresponding to integration of this velocity over one unit of time. On $SO(3)$ the exponential map is given by Rodriquez's formula:

$$\exp\omega = I + \frac{\widehat{\omega}}{\|\omega\|}\sin\|\omega\| + \frac{\widehat{\omega}^2}{\|\omega\|}(1 - \cos\|\omega\|). \tag{11}$$

The rotation matrix $R = \exp\omega$ describes the change in orientation due to rotating with angular velocity ω for one unit of time.

The exponential map on $SE(3)$ can be computed by solving a linear ordinary differential equation, as described in [20]. In homogeneous coordinates the exponential map is given by

$$\exp\begin{bmatrix} v \\ \omega \end{bmatrix} = \begin{bmatrix} \exp\omega & (I - \exp\omega)\dfrac{\omega \times v}{\|\omega\|} + \omega^T v\dfrac{\omega}{\|\omega\|} \\ 0 & 1 \end{bmatrix} \qquad (\omega \neq 0)$$

and

$$\exp \begin{bmatrix} v \\ \omega \end{bmatrix} = \begin{bmatrix} I & v \\ 0 & 1 \end{bmatrix} \qquad (\omega = 0).$$

The exponential map for other subgroups of $SE(3)$ can be computed from these general formulas.

2.3. Principal bundles and connections. In order to formally describe the process of reconstruction, we use the theory of principal fiber bundles and connections. A complete and detailed description of principal bundles can be found in Kobayashi and Nomizu [12]. We restrict ourselves to the simplified class of trivial principal bundles; see also Montgomery [18].

For basic definitions and concepts in differential geometry, we use notation from Boothby [3]. Let M be a smooth manifold of dimension of n. We write T_xM for the tangent space of M at x and $v_x \in T_xM$ for a tangent vector. If $f : M \to N$ is a smooth mapping between manifolds, we write $T_xf : T_xM \to T_{f(x)}N$ to denote the tangent map. A vector field X on M is a smooth mapping $X : M \to TM$ which assigns a tangent vector in T_xM to each point x.

Although we are concerned only with subgroups of the Euclidean group $SE(3)$, it will be convenient to use some more general notation from the theory of Lie groups. If G is a p dimensional (matrix) Lie group, we write $\mathfrak{g}$ to denote the Lie algebra associated with G. As in the last section, we associate $\widehat{\xi} \in \mathfrak{g}$ with a vector $\xi \in \mathbb{R}^p$. If the Lie group G is commutative we say that G is Abelian. In this case the Lie bracket on $\mathfrak{g}$ is zero. We will use the symbol e to denote the identity element of a group.

For every $g \in G$, we define left translation by g as the map $L_g : G \to G$ given by $L_g(h) = gh$ for $h \in G$. Similarly, right translation by g is defined as the map $R_g : G \to G$ satisfying $R_g(h) = hg$. Using the isomorphism between T_eG and $\mathfrak{g}$, we regard T_eL_g as a mapping between $\mathfrak{g}$ and T_gG. Thus the (body) velocity defined in the previous section is written more generally as

$$\widehat{\xi} = (T_eL_g)^{-1}\dot{g} \in \mathfrak{g}$$

Note that for matrix Lie groups $T_eL_g = L_g$ and $T_eR_g = R_g$ as matrices, so we can use matrix multiplication for all mappings.

In studying the locomotion of a robotic system, we will regard the system's internal configuration as a point on a smooth manifold M and its position in ambient space as an element of a Lie group G; the system's complete state space Q will be the Cartesian product of these two submanifolds. Rigid motion of the system with respect to its environment will be given by a *left action* of G on Q. We define this notion in a general setting.

Definition 1. Left action of a group on a manifold
A *left action* of a Lie group G on a manifold Q is a smooth map $\Phi : G \times Q \to Q$ such that

(1) $\Phi(e, q) = q$ for all $q \in Q$;
(2) $\Phi(g_2, \Phi(g_1, q)) = \Phi(g_2g_1, x)$ for every $g_1, g_2 \in G$ and $q \in Q$.

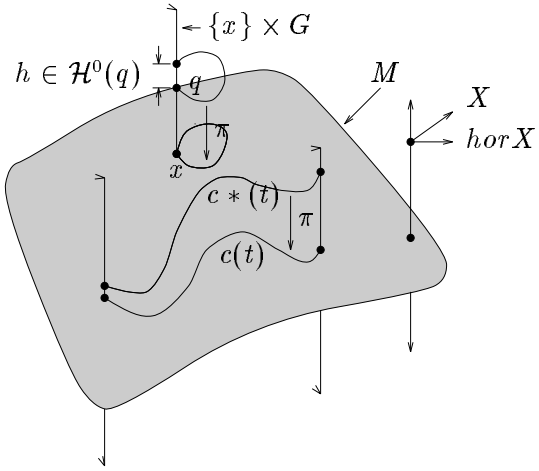

FIGURE 2. Parallel displacement and holonomy in a trivial principal bundle

We sometimes denote $\Phi(g,q)$ by $\Phi_g(q)$. A left action Φ of G on Q is said to be *free* if $\Phi(g,q) = q$ implies that $g = e$ for all $q \in Q$. If Φ is a left action of G on a manifold Q and $\xi \in \mathfrak{g}$, the *infinitesimal generator* of Φ corresponding to ξ is the vector field on Q defined by

$$\xi_Q(q) = \frac{d}{dt}(\Phi(\exp(\widehat{\xi}t), q))\big|_{t=0}. \tag{12}$$

Definition 2. Trivial principal bundle
Let M be a manifold and G a Lie group. A *trivial principal fiber bundle* with *base* M and *structure group* G consists of the manifold $Q = M \times G$ together with a free left action of G on Q given by left translation in the group variable: $\Phi_h(x,g) = (x, hg)$ for $x \in M$ and $g \in G$.

The manifold Q is called the *total space* of the bundle. We denote both the total space and the bundle itself by Q. The set of points $(x_0, g) \in Q$, where x_0 is a particular point in M and $g \in G$, is called the *fiber over* x_0. We denote the projection which carries the points in the fiber over any $x_0 \in M$ to x_0 by $\pi : Q \to M$. We note that nontrivial principal fiber bundles exist, as do principal bundles with structure groups other than those of interest to us.

We define the *vertical subspace* of the principal fiber bundle Q at the point $q \in Q$ to be

$$V_qQ = \{v_q \in T_qQ : v_q = \xi_Q(q) \text{ for some } \xi \in \mathfrak{g}\}. \tag{13}$$

A vector which lies in V_qQ is tangent to the orbit of q under the action of G. Such a vector is said to be *vertical*, or is said to be tangent to the *group* or *fiber direction*. For a trivial principal bundle $Q = M \times G$, the elements of V_qQ have the form $(0, \widehat{\xi}g) \in T_qQ$ for $\widehat{\xi} \in \mathfrak{g}$.

We will model the relevant kinematics of a locomotion system in terms of a *connection* on a principal bundle Q. This notion requires some understanding of

exterior differential forms. A $\mathfrak{g}$-*valued differential p form* on Q is a map which, at any point $q \in Q$, assigns to each set of p vectors $v_1, \ldots v_p \in T_qQ$ an element of $\mathfrak{g}$.

Definition 3. Connection on a principal bundle
A connection Γ on the (trivial) principal bundle $Q = M \times G$ is a $\mathfrak{g}$ valued one form on Q satisfying

(1) $\Gamma(\xi_Q) = \xi$;
(2) $\Gamma(T_q\Phi_g v_q) = \mathrm{Ad}_g\, \Gamma(v_q)$.

Given $v_q \in T_qQ$, $\Gamma(v_q)$ is the unique $\xi \in \mathfrak{g}$ such that $\xi_Q(q)$ is equal to the vertical component of v_q.

A connection Γ on the principal fiber bundle Q assigns to each point $q \in Q$ a *horizontal subspace* H_qQ of T_qQ:

$$H_qQ = \{v_q \in T_qQ : \Gamma(v_q) = 0\}. \tag{14}$$

It follows from the properties of Γ that $T_qQ = H_qQ \oplus V_qQ$ and $H_{\Phi(g,q)}Q = T\Phi_g(H_qQ)$ for $g \in G$. Indeed, given a subspace H_qQ, there is in general a well defined connection such that $H_qQ = \ker \Gamma_q = \{v_q \in T_qQ : \Gamma(v_q) = 0\}$.

Lemma 1. *Let Q be a principal bundle and $H_qQ \subset T_qQ$ a subbundle of the tangent bundle which depends differentiably on q. There exists a connection $\Gamma : TM \to \mathfrak{g}$ with $H_qQ = \ker \Gamma_q$ if and only if*

(1) $T_qQ = H_qQ \oplus V_qQ$;
(2) $H_{\Phi(g,q)}Q = T\Phi_g(H_qQ)$ *for* $g \in G$.

In the context of locomotion systems, the horizontal subspace of a connection will be the set of velocities for which the constraints on the system are satisfied. We will write $\mathrm{hor}(v_q)$ and $\mathrm{ver}(v_q)$ for the projections of v_q onto H_qQ and V_qQ, respectively.

Now assume that a connection has been specified on the bundle Q, and consider the projection map $\pi : Q \to M$. For each $q \in Q$, the associated tangent map $T_q\pi : T_qQ \to T_{\pi(q)}M$ maps the horizontal subspace at q isomorphically onto $T_{\pi(q)}M$. In other words, there is a one-to-one correspondence between vectors in H_qQ and vectors in $T_{\pi(q)}M$. Given a vector $v_x \in T_xM$ and a point q in the fiber over x, there is a unique vector in H_qQ which projects via $T_q\pi$ onto v_x. Given a vector field X on M, there is a unique horizontal vector field X^h on Q which passes through q and projects via $T_q\pi$ onto X. We refer to X^h as the *horizontal lift* of X through q.

Consider now a curve $c(t)$ in M passing through $c(0) = x \in M$. For any given q in the fiber over x, there is a unique curve $c^*(t)$ in Q, called the *horizontal lift* of c, which passes through q, projects to $c(t)$, and is everywhere horizontal: $\frac{d}{dt}c^*(t) \in H_qQ$. If $c(t_1) = x_1$ and $c(t_2) = x_2$, each point q_1 in the fiber over x_1 is connected by a unique horizontal lift of $c(t)$ to a point q_2 in the fiber over x_2. We refer to this map from q_1 to q_2 as *parallel displacement* along $c(t)$. Thus parallel displacement determines a map from $\pi^{-1}(x_1)$ to $\pi^{-1}(x_2)$. We emphasize that horizontal lifting and parallel displacement depend on the choice of connection in the principal fiber bundle Q.

For a trivial principal bundle, the connection one form can always be written as

$$\Gamma(q)\cdot\dot{q} = \mathrm{Ad}_g(\xi + A(x)\cdot\dot{x}) \tag{15}$$

where $\widehat{\xi} = g^{-1}\dot{g}$ and $A : TM \to \mathfrak{g}$. We call the Lie algebra valued form A the *local connection one form.* If X is vector field on TM then the horizontal lift of X is given by

$$X^h(q) = \begin{bmatrix} X(x) \\ -gA(x)\cdot X(x) \end{bmatrix}$$

In the sequel we shall stress the use of $A(x)$ for all computations since it contains all of the information which characterizes the connection.

Consider a point q in the fiber of Q over $x \in M$ and a curve $c : [0,1] \to M$ which both begins and ends at x. Parallel displacement of $\pi^{-1}(x)$ along c maps the point q to some (possibly different) point in $\pi^{-1}(x)$. We recall that the fiber over x is the space $\{x\} \times G$, where G is the structure group of the principal fiber bundle Q.

Definition 4. Geometric phase and holonomy group
The *geometric phase*, or holonomy, of a closed curve $c : [0,1] \to M$ is net change in the group variable determined by the horizontal lift of c. The *holonomy group* of Γ with reference point q consists of the group components of all points in $\pi^{-1}(x)$ reachable from q via parallel translation along loops in M.

The *holonomy bundle* of Γ with reference point q is the set of points in Q which can be joined to q by horizontal curves. We denote the holonomy bundle with reference point q by $Q_{\mathcal{H}}(q)$. Note that $Q_{\mathcal{H}}(q_1) = Q_{\mathcal{H}}(q_2)$ if and only if q_1 and q_2 can be joined by a horizontal curve. The geometric phase is independent of the initial point in the fiber due to the invariance properties of the connection.

If we repeat the construction of the holonomy group with reference point q but restrict ourselves to parallel displacement along contractible loops in the base space M, we obtain the *restricted holonomy group* $\mathcal{H}^0(q)$. Suppose now that we restrict ourselves further to parallel displacement along those contractible loops which are entirely contained in a particular neighborhood U of $x = \pi(q)$. We denote the resulting holonomy group by $\mathcal{H}_U(q)$. The intersection of the groups $\mathcal{H}_U(q)$ for all neighborhoods U of x is called the *local holonomy group* of Γ with reference point q.

Example 1. $M = \mathbb{R}^2$, $G = SE(2)$
Let $Q = \mathbb{R}^2 \times SE(2)$, where $\phi = (\phi_1, \phi_2) \in \mathbb{R}^2$ is a point in the base and $g = (x, y, \theta) \in SE(2)$ is a point in the fiber over ϕ. We take the action of $SE(2)$ on Q to be the standard left action of $SE(2)$ on itself. The infinitesimal generator corresponding to this action can be shown to be

$$\xi_Q = \begin{bmatrix} 0 \\ 0 \\ u - \omega x \\ v + \omega x \\ \omega \end{bmatrix} \qquad \xi = \begin{bmatrix} u \\ v \\ \omega \end{bmatrix} \in se(2). \tag{16}$$

The bundle $Q \in \mathbb{R}^2 \times SE(2)$ is a trivial principal bundle with non-Abelian structure group $SE(2)$. An example of a connection on this bundle is given by

$$\Gamma(q) \cdot v_q = \begin{bmatrix} v_x - a\cos\theta\, v_{\phi_1} + y(v_\theta - b v_{\phi_2}) \\ v_y - a\sin\theta\, v_{\phi_1} - x(v_\theta - b v_{\phi_2}) \\ v_\theta - b v_{\phi_2} \end{bmatrix}.$$

To verify that this is a connection, we first check that $\xi = \Gamma(\xi_Q)$. Using equation (16), we have

$$\Gamma(q) \cdot \xi_Q = \begin{bmatrix} u - \omega y + y\omega \\ v + \omega x - x\omega \\ \omega \end{bmatrix} = \begin{bmatrix} u \\ v \\ \omega \end{bmatrix},$$

as desired. It can be checked similarly that $\Gamma(T_q \Phi_g v_q) = \mathrm{Ad}_g \Gamma(v_q)$. Indeed, we see that the connection form can be written as

$$\Gamma(q) \cdot \dot{q} = \begin{bmatrix} \cos\theta & -\sin\theta & y \\ \sin\theta & \cos\theta & -x \\ 0 & 0 & 1 \end{bmatrix} \left(\begin{bmatrix} v_x \cos\theta + v_y \sin\theta \\ v_x \sin\theta - v_y \cos\theta \\ v_\theta \end{bmatrix} + \begin{bmatrix} -a & 0 \\ 0 & 0 \\ 0 & -b \end{bmatrix} \begin{bmatrix} v_{\phi_1} \\ v_{\phi_2} \end{bmatrix} \right), \tag{17}$$

or

$$\Gamma(q) \cdot \dot{q} = \mathrm{Ad}_g(\xi + A(x) \cdot \dot{x}), \qquad \text{where} \qquad A(x) = \begin{bmatrix} -a & 0 \\ 0 & 0 \\ 0 & -b \end{bmatrix}.$$

$A : TM \to \mathfrak{g}$ is the local connection one form.

3. Constraints, symmetries, and connections

In this section we describe how connections arise in the presence of Pfaffian constraints and symmetries. A more general description of some of this material is available in the paper by Bloch et al. [2]. We also consider some other locomotion systems whose behavior can be modeled approximately using connections.

3.1. Modeling constraints as connections. Consider a mechanical system on a principal bundle $Q = M \times G$ with constraints

$$\omega^a(q) \cdot \dot{q} = 0 \qquad a = 1, \ldots, k,$$

where each ω^a is a one form $\omega^a \in \Omega^1(M)$. Let $\Phi_g : Q \to Q$ represent the action of G on Q and ξ_Q the infinitesimal generator associated with $\xi \in \mathfrak{g}$. We define the two distributions

$$H_q Q = \{v_q \in T_q Q : \omega^a(q) v_q = 0,\, a = 1, \ldots, k\}$$
$$V_q Q = \{\xi_Q \in T_q Q : \xi \in \mathfrak{g}\}.$$

If the constraints are group invariant and $H_q Q \oplus V_q Q = T_q Q$, the constraints define a connection on Q. In this case we can rewrite the constraints in terms of the connection one form:

$$\begin{array}{l} \omega^a(q) \cdot \dot{q} = 0 \\ a = 1, \ldots, k \end{array} \qquad \Longleftrightarrow \qquad \Gamma(q) \cdot \begin{bmatrix} \dot{x} \\ \dot{g} \end{bmatrix} = \mathrm{Ad}_g(\xi + A(x) \cdot \dot{x}) = 0,$$

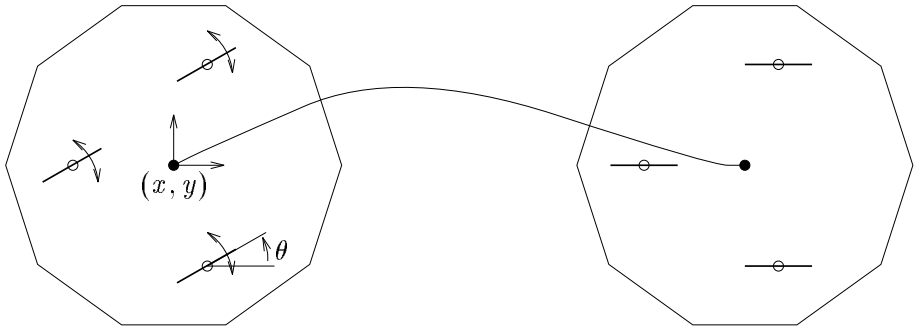

FIGURE 3. Wheeled mobile robot which maintains fixed orientation.

where $\widehat{\xi} = g^{-1}\dot{g}$ and $\Gamma(q) : TQ \to \mathfrak{g}$. The mapping $A : TM \to \mathfrak{g}$ can be represented as a matrix function of $x \in M$ by associating $\mathfrak{g}$ with $\mathbb{R}^p$.

Writing a collection of constraints as a connection one form allows us to express the kinematics associated with these constraints as

$$\dot{g} = -g(A(x) \cdot \dot{x}).$$

We see that the matrix $A(x)$ describes how paths in shape space lift to paths in the group; the basis for locomotion is contained in the geometric content of $A(x)$.

Example 2. *Mobile robot with fixed orientation*
Consider the motion of a mobile robot whose body maintains a fixed orientation with respect to its environs.[1] This is accomplished by a special drive mechanism which turns its three wheels simultaneously around independent axes, as shown in Figure 3. The robot is controlled via this mechanism and a motor which causes the wheels to roll. We let $(x, y) \in \mathbb{R}^2$ denote the position of the center of the robot, $\theta \in S^1$ the steering angle of the wheels, and $\psi \in S^1$ the rotation angle of the wheels as they roll along the ground. We take the radius of the wheels to be ρ.

The motion of this system is constrained by the stipulation that the wheels roll in the direction in which they point without slipping. This set of constraints can be written as

$$\omega^1(q) \cdot \dot{q} = \dot{x}\sin\theta - \dot{y}\cos\theta = 0$$
$$\omega^2(q) \cdot \dot{q} = \dot{x}\cos\theta + \dot{y}\sin\theta - \rho\dot{\psi} = 0.$$

The first equation models the constraint that the wheels can have no velocity perpendicular to the direction in which they point, and the second equation models the constraint that the wheels roll forward without slipping.

We regard the configuration space of the system as a trivial principle bundle $Q = M \times G$ with $(\theta, \psi) \in M = \mathbb{R}^2$ and $(x, y) \in G = (\mathbb{R}^2, +)$. In order to cast the constraints as a connection, we must first verify that the space H_qQ defined by the

[1]One such robot is the B12 Mobile Robot Base, manufactured by Real World Interface, Inc.

constraints satisfies Lemma 1. Setting

$$V_qQ = \{\xi_Q \in T_qQ : \xi \in \mathfrak{g} = \mathbb{R}^2\}$$
$$H_qQ = \{v_q \in T_qQ : \omega^a(a) \cdot q = 0,\ a = 1,2\},$$

we obtain

$$H_qQ = \text{span}\begin{bmatrix} 1 & 0 \\ 0 & 1 \\ 0 & \rho\cos\theta \\ 0 & \rho\sin\theta \end{bmatrix} \qquad V_qQ = \text{span}\begin{bmatrix} 0 & 0 \\ 0 & 0 \\ 1 & 0 \\ 0 & 1 \end{bmatrix}$$

and see immediately that $T_qQ = H_qQ \oplus V_qQ$, and that H_qQ depends differentiably on q. It is also easy to check that $H_{\Phi_g(q)}Q = T\Phi_g(H_qQ)$ since H_qQ is independent of G and $T\Phi_g = I \in \mathbb{R}^{2\times 2}$.

In order to construct the connection one form, we must find a mapping $\Gamma : TQ \to \mathfrak{g}$ which satisfies the conditions in Definition 3 . This one form is determined uniquely by the requirements that $\Gamma(v_q) = 0$ for $v_q \in H_qQ$ and $\Gamma(\xi_Q) = \xi$ for $\xi \in G$. Using these facts, it can be shown that

$$\Gamma(q) \cdot v_q = \begin{bmatrix} v_x - \rho\cos\theta\, v_\psi \\ v_y - \rho\sin\theta\, v_\psi \end{bmatrix}. \tag{18}$$

The local version of the connection, which we shall use for all future calculations, is

$$A(x) = \begin{bmatrix} 0 & -r\cos\theta \\ 0 & -r\sin\theta \end{bmatrix}, \tag{19}$$

where $A(x) : TM \to \mathfrak{g}$.

Example 3. *Two wheeled mobile robot*
The kinematics of the more traditional mobile robot from Section 2 can also be modeled with a connection. If we set $\phi_1 = \frac{1}{2}(\psi_1 + \psi_2)$, $\phi_2 = \frac{1}{2}(\psi_1 - \psi_2)$, and $a = r$, $b = r/l$ in equation (1), the constraints become

$$\begin{aligned} \omega^1 &= v_x\cos\theta + v_y\sin\theta - a v_{\phi_1} \\ \omega^2 &= -v_x\sin\theta + v_y\cos\theta \\ \omega^3 &= v_\theta - b v_{\phi_2}. \end{aligned} \tag{20}$$

These are precisely the equations which appear in equation (17), and it follows that the connection one form

$$\Gamma(q) \cdot v_q = \begin{bmatrix} v_x - a\cos\theta\, v_{\phi_1} + y(v_\theta - b v_{\phi_2}) \\ v_y - a\sin\theta\, v_{\phi_1} - x(v_\theta - b v_{\phi_2}) \\ v_\theta - b v_{\phi_2} \end{bmatrix} \tag{21}$$

models the kinematic constraints (20). The local form of this connection is particularly simple:

$$\Gamma(q)\cdot\dot{q} = \mathrm{Ad}_g(\xi + A(x)\cdot\dot{x}) \qquad A(x) = \begin{bmatrix} -a & 0 \\ 0 & 0 \\ 0 & -b \end{bmatrix}. \tag{22}$$

3.2. Modeling conservation laws as connections. The *mechanical connection* arises in reducing the dynamics of a mechanical system with symmetries. We briefly review the Lagrangian derivation of the mechanical connection here, following the treatment of Bloch et al. [2].

Consider first the case when a system has a set of cyclic variables . Suppose that the Lagrangian $L : TQ \to \mathbb{R}$ for a mechanical system has the form

$$L(q,\dot{q}) = L(r,\dot{r},\dot{s}) \qquad q = (r,s) \in \mathbb{R}^{n-k}\times\mathbb{R}^k.$$

The variables $s \in \mathbb{R}^k$ are said to be *cyclic* since they do not appear in the Lagrangian. Lagrange's equations relative to this splitting of the configuration space are given by

$$\begin{aligned} \frac{d}{dt}\frac{\partial L}{\partial \dot{r}^i} - \frac{\partial L}{\partial r^i} = 0 \qquad & i = 1,\dots,n-k \\ \frac{d}{dt}\frac{\partial L}{\partial \dot{s}^j} = 0 \qquad & j = 1,\dots,k. \end{aligned}$$

If the Lagrangian is the difference between the kinetic and potential energies of the system, the second equation can be written as

$$M_{21}(r)\dot{r} + M_{22}(r)\dot{s} = 0$$

where the M_{ij} are submatrices of the inertia matrix $M(r) \in \mathbb{R}^{n\times n}$. This equation has the same form as a Pfaffian constraint, and if the Lagrangian is nondegenerate we can write

$$\dot{s} = -M_{22}^{-1}M_{21}\dot{r}.$$

This equation is exactly the horizontal lift of a connection

$$\Gamma(q)\cdot\dot{q} = \dot{s} + M_{22}^{-1}M_{21}\dot{r}$$

on the Abelian principal bundle $\pi : \mathbb{R}^n \to \mathbb{R}^{n-k}$ with $G = \mathbb{R}^k$ and addition as the group operation.

In a more general context we rely on Noether's theorem to define a connection. Let $L : TQ \to \mathbb{R}$ be a simple Lagrangian (kinetic energy minus potential) and suppose there exists a Lie group G and an action $\Phi : G\times Q \to Q$ such that

$$L(\Phi_g(q), T_q\Phi_g\cdot\dot{q}) = L(q,\dot{q})$$

for all $g \in G$, $q \in Q$, and $\dot{q} \in T_qQ$. If this is the case we say that L is G *invariant.* Noether's theorem asserts that conserved quanities exist whenever L is G invariant:

Theorem 1 (Noether). *Let $L : TQ \to \mathbb{R}$ be a G invariant Lagrangian of a system whose dynamics are described by Lagrange's equations. The vector function $J : TQ \to \mathfrak{g}^*$ defined by*

$$\langle J(q,\dot{q}),\, \xi\rangle = \langle \frac{\partial L}{\partial \dot{q}}(q,\dot{q}),\, \xi_Q(q)\rangle \qquad \xi \in \mathfrak{g}$$

is constant along trajectories of the system.

The most common examples of conserved quantities are linear and angular momentum, corresponding to $G \in \mathbb{R}^3$ and $G = SO(3)$ respectively. If a conserved quantity is identically zero and we write the components of ξ_Q as $K_a^i \xi^a$, we can write the components of J as

$$\omega_a(q) \cdot \dot{q} = J_a(q,\dot{q}) = K_a^i M_{ij} \dot{q}^j = 0,$$

which once again has the form of a Pfaffian constraint.

The mapping $J : TQ \to \mathfrak{g}^*$ maps velocities to the dual of the Lie algebra. To obtain a connection (which takes values in $\mathfrak{g}$), we define the *locked inertia tensor* $I(q) : \mathfrak{g} \to \mathfrak{g}^*$ to be the unique mapping which satisfies

$$\langle I\xi, \eta\rangle = \xi_Q^T M(q) \eta_Q \qquad \xi, \eta \in \mathfrak{g}.$$

We can then define a mapping $\Gamma(q) : TQ \to \mathfrak{g}$ such that

$$\Gamma(q) \cdot \dot{q} = I^{-1}(q) J(q,\dot{q}) = I^{-1}(q) K(q) M(q) \dot{q}.$$

It can be shown that Γ is a connection on the (possibly nontrivial) bundle $\pi : Q \to Q/G$; it is called the *mechanical connection*. The mechanical connection can be used to model the motion of systems which obey conservation laws, as illustrated in the next example.

Example 4. *Planar space robot*

Figure 4 shows a simplified model of a planar robot consisting of two arms connected to a central body via revolute joints. If the robot is free floating, then the law of conservation of angular momentum implies that motion of the arms can cause the central body to rotate. If the angular momentum is zero, this conservation law can be viewed as a Pfaffian constraint on the system.

Let θ be the angle of the central body with respect to the horizontal, ψ_1 and ψ_2 the angles of the left and right arms with respect to the central body, m the mass of each of the arms, and J the inertia of the central body. The kinetic energy of the system has the form

$$K = \frac{1}{2} \begin{bmatrix} \dot{\psi}_1 \\ \dot{\psi}_2 \\ \dot{\theta} \end{bmatrix}^T \begin{bmatrix} ml^2 & 0 & ml^2 + m\rho\cos\psi_1 \\ 0 & ml^2 & ml^2 + m\rho\cos\psi_2 \\ ml^2 + m\rho\cos\psi_1 & ml^2 + m\rho\cos\psi_2 & \begin{matrix} J+2ml^2+2m\rho^2+ \\ 2m\rho l(\cos\psi_1+\cos\psi_2) \end{matrix} \end{bmatrix} \begin{bmatrix} \dot{\psi}_1 \\ \dot{\psi}_2 \\ \dot{\theta} \end{bmatrix}.$$

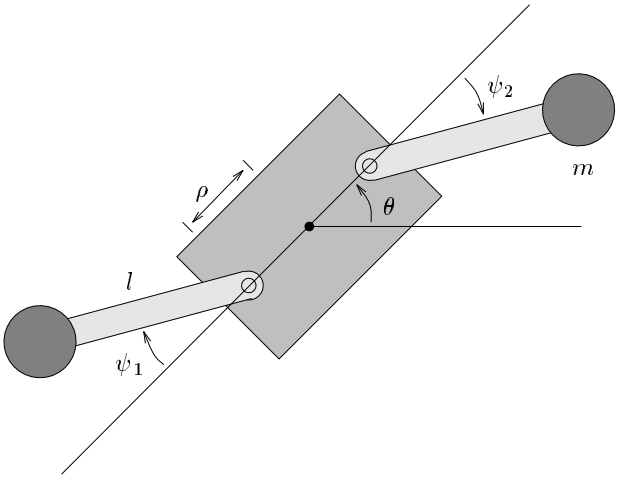

FIGURE 4. A simplified model of a planar space robot.

Note that the kinetic energy of the system is independent of the variable θ. It therefore follows from Lagrange's equations that in the absence of external forces,

$$\frac{d}{dt}\frac{\partial L}{\partial \dot{\theta}} = -\frac{\partial L}{\partial \theta} = 0.$$

Thus the quantity $\partial L/\partial \dot{\theta}$ is a constant of the motion. This is precisely the angular momentum, μ, of the system:

$$\mu = \frac{\partial L}{\partial \dot{\theta}} = (ml^2 + m\rho\cos\psi_1)\dot{\psi}_1 + (ml^2 + m\rho\cos\psi_2)\dot{\psi}_2 + (J + 2ml^2 + 2m\rho^2 + 2m\rho l(\cos\psi_1 + \cos\psi_2))\dot{\theta}. \quad (23)$$

If the initial angular momentum is zero, then *conservation of angular momentum* ensures that it stays zero.

To put this in the framework of connections, we choose ψ_1 and ψ_2 to be the base variables and θ to be the fiber variable. Thus $M = S^1 \times S^1$ and $G = S^1$ with addition mod 2π as the group operation. The connection defined by the constraint is given by

$$\Gamma(q)\cdot v_q = v_\theta + \frac{ml^2 + m\rho\cos\psi_1}{(J + 2ml^2 + 2m\rho^2 + 2m\rho l(\cos\psi_1 + \cos\psi_2))} v_{\psi_1} + \frac{ml^2 + m\rho\cos\psi_2}{(J + 2ml^2 + 2m\rho^2 + 2m\rho l(\cos\psi_1 + \cos\psi_2))} v_{\psi_2}. \quad (24)$$

3.3. Other systems. Other types of locomotion systems can be modeled, at least approximately, using connections on principal bundles. We require that the motion of such systems be determined exclusively by their kinematics, without dynamic terms. We illustrate with the example below and those in Section 5.

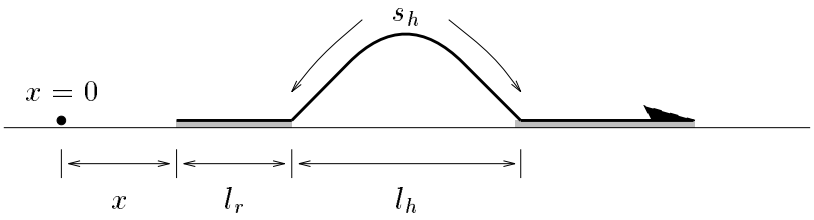

FIGURE 5. Simple model for an inchworm robot

Example 5. *Inchworm robot*
We begin with a simple model for the linear locomotion of a snakelike robot of unit length, as depicted in Figure 5. This system is visually reminiscent of a crawling inchworm, although we make no attempt here to construct a biologically accurate model of inchworm locomotion (such as that presented in Keller and Falkovitz [11]). The variable l_r denotes the length of the rear segment in contact with the ground, s_h the arc length of the raised segment, or *hump*, and l_h the hump's longitudinal span. Segments in contact with the ground share a constant uniform thickness. The robot is aligned with the x axis.

If we assume viscous friction where the robot comes in contact with the plane, sliding motion of a segment of the robot will be opposed by a force proportional to both the sliding velocity and the length of the contact segment. In the absence of inertial effects, the locomotion of the robot will be governed by the requirement that it experience zero net viscous drag at all times. This is reflected in the equation

$$l_r\dot{x} + (1 - l_r - s_h)(\dot{x} + \dot{l}_h - \dot{s}_h) = 0. \tag{25}$$

We regard the shape space of this system as an open subset of $\mathbb{R}^3$; the preceding equation defines the connection

$$\Gamma(q) \cdot v_q = \dot{x} + \frac{(1 - l_r - s_h)}{(1 - s_h)}(\dot{l}_h - \dot{s}_h) \tag{26}$$

on the bundle over this space with structure group $(\mathbb{R}, +)$.

Although we have obtained this connection from a viscous friction model, we will find in the next section that it affords us insight into the robot's behavior subject to a broader class of models. If, specifically, the robot never exerts a tangential force along its contact with the ground, the nature of the opposing frictional force is somewhat irrelevant. Under certain gait assumptions, then, computations of geometric phase based on equation (26) will remain valid in the presence of more biologically accurate friction models.

The theory of connections has also been applied to the study of swimming motions for biological organisms. Shapere and Wilczek showed that the motion of paramecia could be described using a connection derived from the basic laws of low Reynolds number hydrodynamics [26]. The interested reader should note that some of their results are presented in the language of gauge theory; their terminology and ours are developed in parallel by Bleeker [1].

4. Generating motion using geometric phases

In this section we study the motion of a system which executes a loop in the shape space and the analyze the *controllability* of the system; we seek conditions under which we can steer a system to an arbitrary location in $SE(3)$ or one of its subgroups.

Suppose that the kinematics of a locomotion system can be modeled as a connection on the trivial principal bundle $Q = M \times G$. As a control problem, the system's kinematics can be written as

$$\dot{q} = X_1^h u^1 + \cdots + X_m^h u^m \qquad \{X_1, \ldots, X_m\} \in TM \subset TQ. \tag{27}$$

If X_i is a vector field on the base space M which corresponds to a control, flow along X_i in M lifts to flow along the vector field X_i^h in Q. If we let (x, g) be coordinates for the base and group, equation (27) can be written as

$$\begin{bmatrix} \dot{x} \\ \xi \end{bmatrix} = \begin{bmatrix} I \\ A(x) \end{bmatrix} u, \tag{28}$$

where we represent $A : TM \to \mathfrak{g}$ as a matrix and $\widehat{\xi} = g^{-1}\dot{g}$.

Our goal is to study the controllability of the system described by equation (27) in terms of the properties of the local connection form $A(x)$. This has the advantage of properly taking into account the role of the Lie group G, and the avoids the use of local coordinates, which can lead to extremely messy formulas.

4.1. Basic definitions. We now make precise the notion of controllability for a locomotion system. There are two cases to consider: controllability on the entire space $Q = M \times G$ and controllability only on the fibers.

Definition 5. Strong controllability
A locomotion system is said to be *strongly controllable* if, for any $q_0 = (x_0, g_0)$ and $q_f = (x_f, g_f)$, there exists a time $T > 0$ and a curve $x(\cdot)$ connecting x_0 and x_f in the base space such that the horizontal lift of x passing through q_0 satisfies $x^*(0) = q_0$ and $x^*(T) = q_f$.

For many locomotion systems we are not necessarily interested in strong controllability, since we may not care about the final configuration of the base variables. These include the mobile robots in Examples 2 and 3, where base variables corresponded to the internal angles of the wheels. In studying such systems, we make use of a weaker notion of controllability:

Definition 6. Weak controllability
A locomotion system is said to be *weakly controllable* if, for any initial position $g_0 \in G$, final position $g_f \in G$, and initial shape $x_0 \in M$, there exists a time $T > 0$ and a base space curve $x(\cdot)$ satisfying $x(0) = x_0$ such that the horizontal lift of x passing through (x_0, g_0) satisfies $x^*(0) = q_0$ and $x^*(T) = (x(T), g_f)$.

For both strong controllability and weak controllability, we will make extensive use of the geometric phase, or holonomy, associated with a closed path in the base space. A connection on the trivial principal bundle $M \times G$ uniquely determines a system's trajectory in the full space from a loop C in the base space. Since the system's velocity remains horizontal, the base and fiber components $\dot{x}$ and $\dot{g}$ of its velocity satisfy

$$\dot{g}(t) = -g(A(x) \cdot \dot{x}). \tag{29}$$

Integrating this equation with the initial condition $g(0) = e$, we obtain the geometric phase corresponding to the closed curve $C \subset M$.

In particular, if the holonomy group of the connection is rich enough, we can use the following algorithm to steer from an initial configuration q_0 to a final configuration q_f:

> *Step 1.* Choose a time $T_1 > 0$ and a path $x(t)$ such that $x(0) = x_0$ and $x(T_1) = x_f$. Let $g(T_1)$ be the corresponding value of the group variable, as determined by integrating equation (29).
>
> *Step 2.* Choose a closed one dimensional curve $C \subset M$ such that the geometric phase associated with C is given by $g_f(g(T_1))^{-1} \in G$.

If a system is strongly controllable this basic algorithm will always work, although it may not yield optimal paths.

4.2. Area rules. The differential equation (29) cannot generally be integrated in closed form. However, if G is an Abelian Lie group, the integral can be simplified considerably. Assume that $x(t) \in C$ is chosen such that x traverses C in one unit of time. It can be shown that in the Abelian case, the solution to equation (29) can be written as

$$g(1) = \exp\left(\int_0^1 (-A(x) \cdot \dot{x})dt\right) g(0). \tag{30}$$

In other words, in the Abelian case we can integrate the Lie algebra valued quantity $A(x) \cdot \dot{x}$ along the curve and then exponentiate the resulting Lie algebra element to obtain the net motion in the fiber.

The line integral in equation (30) can be further simplified by converting it into a surface integral, using the generalized Stokes theorem [3]. Let $C = \partial S$ be a closed, oriented curve in a manifold M which bounds a p dimensional region $S \subset M$, and let ω be a smooth p form on S; then

$$\int_{\partial S} \omega = \int_S d\omega. \tag{31}$$

This equation also holds if ω is vector valued by applying it to each of the components of the vector valued form.

The mapping $A(x) : TM \to \mathfrak{g}$ is a vector-valued form over the base and we can therefore rewrite (30) as

$$g(1) = \exp\left(-\int_C A(x)\right).$$

According to Stokes' theorem, the net holonomy is

$$g(1) = \exp\left(-\int_C A(x)\right) g(0) = \exp\left(-\iint_S dA(x)\right) g(0), \tag{32}$$

where S is any surface such that $C = \partial S$. Equation (32) is called the *area rule* for computing geometric phase. It asserts that in a principal bundle with an Abelian structure group and a given connection, the holonomy associated with a base space curve C is equal to the appropriately weighted area of any surface bounded by C.

We can use this basic result to characterize the controllability of locomotion systems modeled via connections on Abelian principal bundles.

Proposition 2. Strong controllability of Abelian locomotion systems
A locomotion system on an Abelian principal bundle is strongly controllable if and only if

$$\text{span}\{dA(X,Y) : X, Y \in T_xM, x \in M\} = \mathfrak{g}.$$

This proposition is actually a special case of the Ambrose-Singer theorem presented in the next subsection. Notice that the span in the proposition is taken over *all* base points $x \in M$. The reason for this is seen in the second example below.

Example 6. *Inchworm robot*
Consider the snakelike robot described in Example 5 of the last section. Figure 6 depicts a gait which recalls the rectilinear motion of a caterpillar. The robot lifts and buckles its trailing end, replacing its hind tip with some forward displacement. The arched segment then passes the length of the robot to lift the forward tip, and the robot re-extends in its new location. At no point does any portion of the robot drag along or exert a tangential force upon the ground. Because our parametrization of the robot's shape suggests constant contact with the ground at both ends, we regard the lifted buckling and unbuckling motions as if segments of zero length were being dragged.

If the snake assumes the sequence of configurations represented in Figure 6(a) in the manner indicated by the arrows, the net linear displacement of its rearmost point is

$$x(1) = \exp\Big(-\int_C A(x)\Big).$$

Since

$$\int_C A(x) = \int_C \left(\frac{(1 - l_r - s_h)}{(1 - s_h)}\right)(dl_h - ds_h) = \int_{1/3}^{1/6} dl_h = -\frac{1}{6} \tag{33}$$

and the exponential map on $\mathbb{R}$ is just the identity, the net motion is

$$x(1) = \frac{1}{6}.$$

The sequence of shapes assumed by the robot during this maneuver is depicted in Figure 6(b). Since we measure the robot's progress in terms of the displacement of

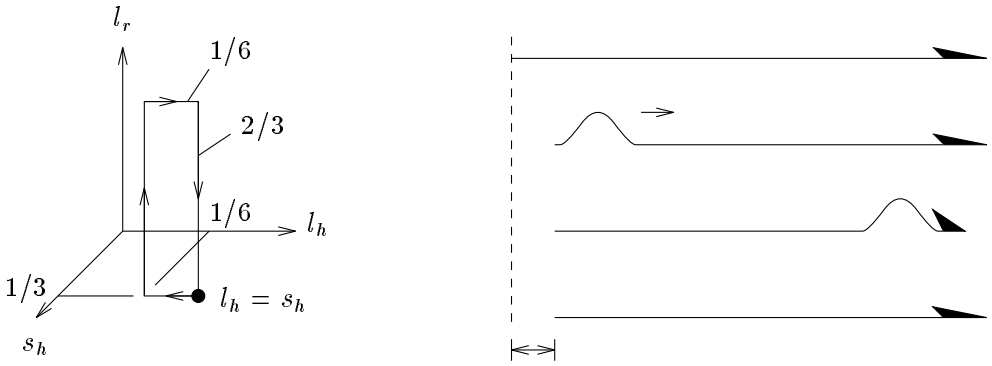

(a) (b)

FIGURE 6. Caterpillar gait

its hind tip, the integrals corresponding to three of this maneuver's four stages are identically zero. Notice that s_h remains constant throughout.

We can also compute the net motion of the snake with the area rule. The exterior derivative of A is given by

$$\begin{aligned} dA(x) &= d\left(\frac{(1-l_r-s_h)}{(1-s_h)}\right) \wedge (dl_h - ds_h) \\ &= \frac{1}{1-s_h}(-dl_r \wedge dl_h + dl_r \wedge ds_h + \frac{l_r}{1-s_h} dl_h \wedge ds_h,) \end{aligned} \tag{34}$$

and the holonomy for the path shown in Figure 6(a) is

$$\begin{aligned} x(1) &= \exp\left(-\iint_S \frac{1}{1-s_h}\, dl_h \wedge dl_r\right) \\ &= \exp\left(\int_{1/6}^{1/3}\int_0^{2/3} \frac{3}{2}\, dl_r dl_h\right) = \exp(1/6) = 1/6. \end{aligned} \tag{35}$$

Note that the quantity dA provides a measure of performance in the sense that larger displacements are realized when regions in which dA is large are enclosed.

Example 7. *Mobile robot with fixed orientation*
As a second example, we consider the motion of the mobile robot from Example 2. The local connection form is given by

$$A = \begin{bmatrix} -r\cos\theta\, d\psi \\ -r\sin\theta\, d\psi \end{bmatrix}$$

and its exterior derivative by

$$dA = \begin{bmatrix} r\sin\theta\, d\theta \wedge d\psi \\ -r\cos\theta\, d\theta \wedge d\psi \end{bmatrix}.$$

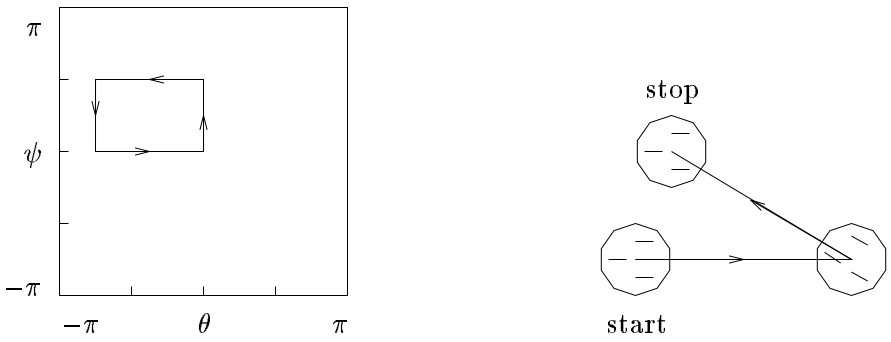

(a) (b)

FIGURE 7. Simple motion for Alfred

We see that this system is strongly controllable by choosing $\theta = 0$ and $\theta = \pi/2$ and taking the span of dA over all vectors fields in the base.

If we begin at the origin and integrate dA around a rectangle of length a in θ and length b in ψ, as shown in Figure 7, the net motion in x and y is

$$\begin{bmatrix} x(1) \\ y(1) \end{bmatrix} = \begin{bmatrix} x(0) \\ y(0) \end{bmatrix} + \begin{bmatrix} br(1 - \cos a) \\ -br \sin a \end{bmatrix}. \tag{36}$$

Notice that the mapping from a, b to points in $\mathbb{R}^2$ is *not* surjective. In particular, if we require that $y(1) = y(0)$, then by necessity either $b = 0$ or $a = 2\pi k$ for some integer k, and in these cases we also get $x(1) = x(0)$. It might appear, then, that this system contradicts Proposition 2, since we cannot steer, for example, from $q_0 = (0, 0, 0, 0)$ to $q_f = (0, 0, x_f, 0)$ if $x_f \neq 0$.

The problem is resolved understanding the necessity for taking the range of dA over *all* base points. Intuitively, we see that if we wish to move in the direction in which the wheels point, it is not possible in general to do this via a closed path in the ψ variable since ψ/ρ measures the distance traveled. Instead, we turn the wheels sideways (to $\theta = \pi/2$) and "wiggle" in the x direction in a cyclic fashion. At $\theta = \pi/2$ we compute

$$dA = \begin{bmatrix} rd\theta \wedge d\psi \\ 0 \end{bmatrix},$$

so infinitesimal loops around $\pi/2$ do indeed generate the motion desired.

This system brings to light a limitation of the area rule for systems on Abelian principal bundles. Stokes' theorem (and hence the area rule) rely on the use of closed loops in M which bound surfaces $S \subset M$. For base spaces which are not simply connected, it is possible to have non-contractable loops which do not bound any surface. Motion in ψ from 0 to 2π with θ fixed at 0 determines such a "loop", describing a circle around one section of the torus $S^1 \times S^1$. In cases such as this, we must rely on the line integral (30) to compute the holonomy associated with a loop.

4.3. Controllability and Curvature. The area rule allows us to characterize the controllability of a system on an Abelian principal bundle.. Unfortunately, for generic locomotion in the plane and elsewhere, the structure group is not Abelian and the preceding formulas cannot be applied. We now consider the more general case, relying again on the concept of geometric phase, or holonomy. The geometric object of central interest will be the curvature of a connection.

Definition 7. Curvature of a connection
Given a connection form Γ on Q, we define the corresponding *curvature form* to be the $\mathfrak{g}$-valued differential two form $D\Gamma$ satisfying

$$D\Gamma(v_1, v_2) = d\Gamma(\text{hor}\, v_1, \text{hor}\, v_2) \tag{37}$$

for $v_1, v_2 \in T_qQ$.

Note that $\Omega(v_1, v_2) = 0$ if either of the tangent vectors v_1, v_2 is vertical. In practice, we often obtain the curvature of a connection via the *structure equation*

$$D\Gamma(v_1, v_2) = d\Gamma(v_1, v_2) - [\Gamma(v_1), \Gamma(v_2)], \tag{38}$$

where $[\cdot, \cdot]$ denotes the Lie bracket on $\mathfrak{g}$. Recall that when G is an Abelian Lie group, the Lie bracket of any two elements of the corresponding Lie algebra is identically zero. In the Abelian case, then, the structure equation becomes

$$D\Gamma(v_1, v_2) = d\Gamma(v_1, v_2) \qquad \text{(Abelian case)}. \tag{39}$$

The relationship between controllability and curvature is given by the Ambrose-Singer theorem.

Theorem 3 (Ambrose-Singer). *Let Q be a principal bundle with structure group G over a connected manifold M. Let Γ be a connection in Q, $D\Gamma$ its curvature, $\mathcal{H}(q)$ the holonomy group with reference point $q \in Q$, and $Q_{\mathcal{H}}(q)$ the holonomy bundle with reference point q.. Then the Lie algebra of $\mathcal{H}(q)$ is equal to the subspace of $\mathfrak{g}$, the Lie algebra of G, spanned by all elements of the form $D\Gamma_p(u, v)$, where $p \in Q_{\mathcal{H}}(q)$ and u and v are horizontal vectors at p.*

The Ambrose-Singer theorem completely characterizes controllability, but requires that we evaluate the curvature form at all *reachable* points of a system, which is precisely what we are trying to determine. We can reformulate the controllability problem using a classical theorem describing local controllability for driftless control systems. A locomotion system may be regarded as the control system

$$\dot{q} = X_1^h u^1 + \cdots + X_m^h u^m, \tag{40}$$

where $X_1, \ldots, X_m$ are vector fields on M. We assume the vector fields X_i^h to be linearly independent and smooth. We say that this system is *locally controllable* at $q \in Q$ if the set points which can be reached by varying the inputs u contains an open neighborhood of q.

Theorem 4 (Chow). *The control system* (40) *is locally (strongly) controllable if and only the vector fields* X_i^h *and all their iterated Lie brackets of all orders span* T_qQ.

To determine controllability we need merely compute a sufficient selection of these brackets. The extra structure present in the principal bundle case simplifies these computations. Define the following sequence of subspaces of the Lie algebra $\mathfrak{g}$ at a fixed point $x \in M$:

$$\begin{aligned}
\mathfrak{h}_1 &= \text{span}\{A(X) : X \in T_xM\} \\
\mathfrak{h}_2 &= \text{span}\{DA(X,Y) : X, Y \in T_xM\} \\
\mathfrak{h}_3 &= \text{span}\{L_Z DA(X,Y) - [A(Z), DA(X,Y)], [DA(X,Y), DA(W,Z)] : W, X, Y, Z \in T_M\} \\
&\vdots \\
\mathfrak{h}_k &= \text{span}\{L_X \xi - [A(X), \xi], [\eta, \xi] : X \in T_xM, \xi \in \mathfrak{h}_{k-1}, \eta \in \mathfrak{h}_2 \oplus \cdots \oplus \mathfrak{h}_{k-1}\}.
\end{aligned} \tag{41}$$

Proposition 5. Strong and weak controllability of locomotion systems
A system defined on a trivial principal bundle Q *over* M *with structure group* G *and local connection* $A(x)$ *is* locally weakly controllable *near* $q \in Q$ *if and only if*

$$\mathfrak{g} = \mathfrak{h}_1 \oplus \mathfrak{h}_2 \oplus \mathfrak{h}_3 \oplus \cdots .$$

The system is locally strongly controllable *if and only if*

$$\mathfrak{g} = \mathfrak{h}_2 \oplus \mathfrak{h}_3 \oplus \cdots .$$

We present a proof of this proposition in Appendix A.

Example 8. *Two wheeled mobile robot*
The local connection form for the two wheeled mobile robot of Example 3 is

$$A = \begin{bmatrix} -a\, d\phi_1 \\ 0 \\ -b\, d\phi_2 \end{bmatrix},$$

and the local curvature form is

$$DA(x) = dA - [A, A] = 0 - \begin{bmatrix} 0 \\ ab\, d\phi_1 \wedge d\phi_2 \\ 0 \end{bmatrix}.$$

The vectors

$$A \cdot \begin{bmatrix} 1 \\ 0 \end{bmatrix} = \begin{bmatrix} -a \\ 0 \\ 0 \end{bmatrix} \quad \text{and} \quad A \cdot \begin{bmatrix} 0 \\ 1 \end{bmatrix} = \begin{bmatrix} 0 \\ 0 \\ -b \end{bmatrix}$$

span $\mathfrak{h}_1$, and the vector

$$DA \cdot \left(\begin{bmatrix} 1 \\ 0 \end{bmatrix}, \begin{bmatrix} 0 \\ 1 \end{bmatrix} \right) = \begin{bmatrix} 0 \\ -ab \\ 0 \end{bmatrix}$$

spans $\mathfrak{h}_2$. Since these three vectors are linearly independent, the system is weakly controllable. Since these are all constant vectors and the third component of the Lie bracket of any two elements of $se(2)$ is zero, no element of $\mathfrak{h}_k$, $k = 3, 4, \ldots$, will have a nonzero third component. The system cannot, therefore, be strongly controllable.

We now use the curvature form to define the infinitesimal holonomy group at a point $q \in Q$. Let $m_k(q)$ be the subspace of $\mathfrak{g}$ spanned by all elements of the form

$$L_{V_1} \cdots L_{V_k} D\Gamma(X, Y),$$

where X, Y, and $V_1 \ldots V_k$ are horizontal vector fields at q. The *infinitesimal holonomy group* with reference point q is defined to be the Lie group generated by the union $\mathfrak{h}_{inf}(q)$ of all $m_k(q)$, $k = 0, 1, \ldots$. The infinitesimal holonomy group $\mathcal{H}_{inf}(q)$ is a subgroup of the local holonomy group $\mathcal{H}_{loc}(q)$ at any $q \in Q$. If the dimension of $\mathcal{H}_{inf}$ is constant throughout a neighborhood of $q \in Q$, then $\mathcal{H}_{inf}(q)$ and $\mathcal{H}_{loc}(q)$ are equal; if the dimension of $\mathcal{H}_{inf}$ is constant in all of Q then $\mathcal{H}_{inf}(q) = \mathcal{H}_{loc}(q) = \mathcal{H}^0(q)$. These facts are proven in Kobayashi and Nomizu [12].

Corollary 6. *If the infinitesimal holonomy group $\mathcal{H}_{inf}(q)$ corresponding to a locomotion system on an Abelian principal bundle Q has constant dimension in Q, the system is locally strongly controllable if and only if $\mathfrak{h}^0(r, e) = \mathfrak{g}$.*

In other words, we can steer the system between any two points in configuration space if and only if we can achieve arbitrary motion in the fiber direction via contractible loops in the base space. This follows from the fact that $\mathfrak{h}_{inf}(q)$ is precisely the direct sum $\mathfrak{h}_2 \oplus \mathfrak{h}_3 \oplus \cdots$ in the Abelian case.

4.4. Integrally related sinusoids and gaits. We now concentrate on specific methods for generating motion through cyclic changes in a robot's shape. The repetition of a particular sequence of shapes defines a *gait*.

Definition 8. Gaits
A *gait* for a locomotion system whose kinematics are modeled by a connection on the trivial principal bundle $Q = M \times G$ is any closed path in M. A gait is said to be a *simple* gait if the closed path can be smoothly deformed to a point.

We may categorize gaits in a variety of ways. Closed paths which are restricted to the same submanifold of shape space may, for instance, be regarded as qualitatively similar. We may instead differentiate a "turning gait" from one which generates rectilinear motion, according to function rather than form. Refining the latter perspective, we refer to walking, trotting, and running as different quadruped gaits.

We associate each different closed path in the base space with a different gait, and isolate a particular equivalence classes of closed paths under continuous deformation. Of course, there are an infinite number of equivalence classes of curves; we frequently desire a finite classification of gaits. It is not clear *a priori* whether or not the quadruped gaits named above represent equivalence classes of curves.

A system's full complement of gaits is often well represented, at least qualitatively, by the set of those which correspond to oriented Lissajous figures in shape space.

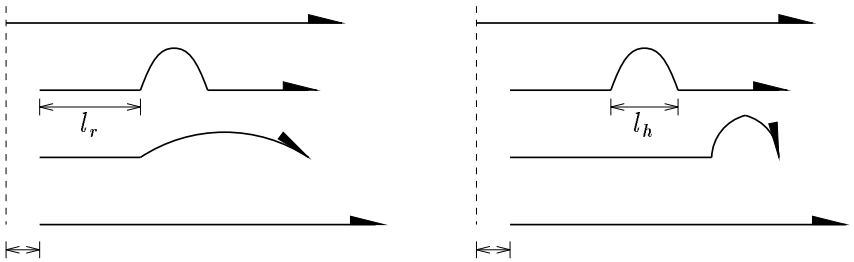

(a) l_r constant (b) l_h constant

FIGURE 8. More gaits for the inchworm robot

In each of the examples below, we focus on gaits which are realized when a system's shape variables vary sinusoidally with integrally related frequencies. The phase differences among the variations in different parameters, as well as their relative frequencies, distinguish particular gaits.

Example 9. *Inchworm robot*
The so-called "caterpillar" gait depicted in Figure 6 is representative of the class of gaits which leaves the shape variable s_h fixed. Figures 8(a) and (b) portray cyclic shape changes which leave l_r and l_h fixed, respectively. We now explore graphically the range of gaits corresponding to planar loops in shape space. Since the majority of these gaits rely specifically on our friction model to generate holonomy, we do not expect them to have counterparts in nature. However, for robotic mechanisms these gaits are representative when the frictional forces are dominated by viscous terms.

Consider the vector

$$u(t) = \begin{bmatrix} \frac{1}{8}\cos t \\ \frac{1}{8}\sin t \\ 0 \end{bmatrix}.$$

This is a parametrization in $t \in [0, 2\pi]$ of a circular loop in shape space, centered about the origin and lying in the plane perpendicular to the s_h axis. Let us assign to each point on the unit sphere the analogous loop in the plane perpendicular to its coordinate vector; we orient this assignment such that the loop given above corresponds to the pole $(l_r, l_h, s_h) = (0, 0, 1)$. Each loop defines a cyclic variation in shape; we compute in each case the system's net translation given

$$\begin{bmatrix} l_r(0) \\ l_h(0) \\ s_h(0) \end{bmatrix} = \begin{bmatrix} 3/16 \\ * \\ 1/2 \end{bmatrix}$$

and

$$\begin{bmatrix} dl_r/dt \\ dl_h/dt \\ ds_h \end{bmatrix} = \frac{1}{8} R \begin{bmatrix} \cos t \\ \sin t \\ 0 \end{bmatrix} \qquad t \in [0, 2\pi],$$

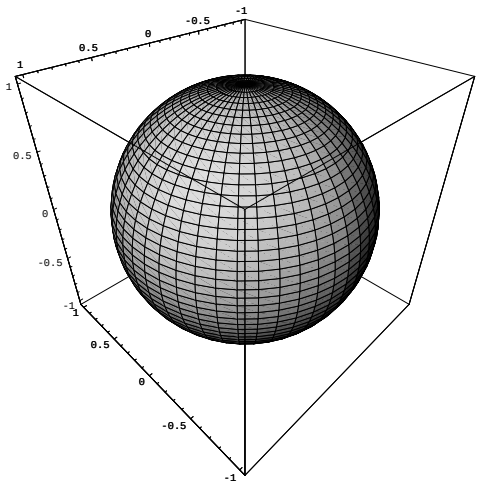

FIGURE 9. Geometric phase of different gaits for the inchworm robot. The lighter areas correspond to more efficient gaits.

where $R \in SO(3)$ denotes the appropriate rotation matrix. The lighter points in Figure 9 correspond to displacements of greater magnitude, the darker points to less efficient gaits. Antipodal points correspond to equal displacements in opposite directions, since reflection through the origin corresponds to path reversal in the base space.

Example 10. *Mobile robot with fixed orientation*
For the mobile robot with fixed orientation, we observe a variety of gaits when the shape parameters θ and ψ are varied sinusoidally with integrally related frequencies. A few are depicted in Figure 10. These show that it is possible to change the robot's orientation and displace it sideways by choosing curves in the base space which enclose appropriate areas.

There are many other robotic systems for which integrally related sinusoids can be used to achieve motion. In [21], Murray and Sastry explored the use of sinusoidal inputs to control a kinematic model of a car, a hopping robot, and a car with trailers. More complicated examples of sinusoidal gaits can be found in the paper by Lewis et al [14], which explores gaits for the "snakeboard", a variant of the skateboard which exploits the coupling of rolling constraints and conservation-like laws to achieve motion.

5. EXAMPLES

We now present some longer examples to illustrate how the ideas presented here can be applied to different robotic systems.

5.1. Kinematic car. Figure 11 depicts a kinematic model of an automobile on the plane. For simplicity's sake, we treat the front and rear pairs of wheels as single wheels at the midpoints of their respective axles. We parametrize the shape space $M \subset S^1 \times S^1$ by the steering angle ϕ and the rotation angle ψ of the rear wheel.

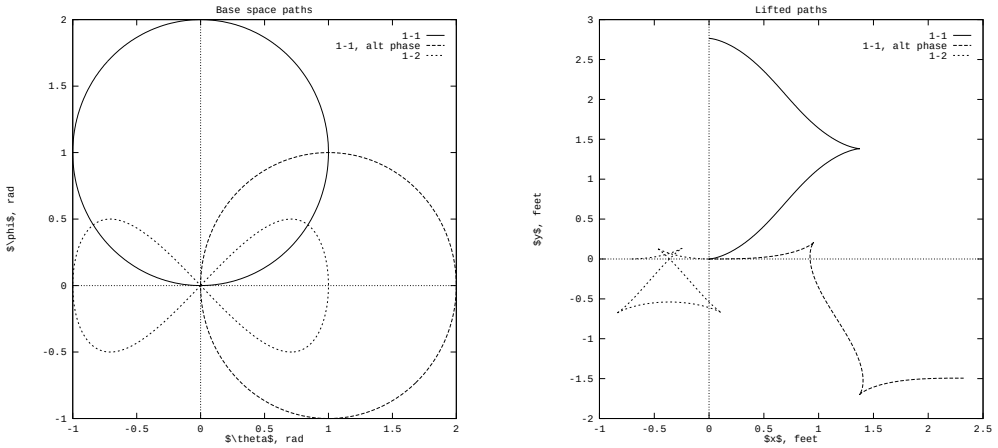

(a) (b)

FIGURE 10. Different types of gaits for a mobile robot with fixed orientation.

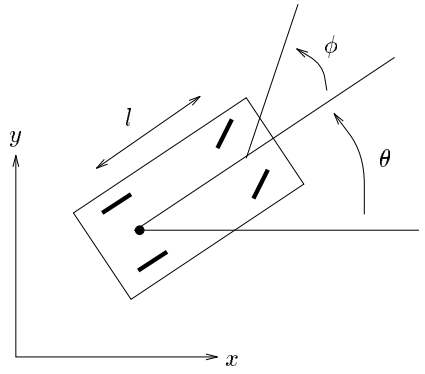

FIGURE 11. A simple model of an automobile.

We control the system by specifying these angles for all time; we will not need the rotation angle of the front wheel. We define ψ to increase as the car moves forward. We denote the radius of the wheels by ρ and the distance between their centers by l.

Motion of the car is restricted at any point by the specification that the wheels can roll but cannot slide on the plane. Since neither wheel can slide transverse to its rolling direction,

$$\dot{x}\sin\theta - \dot{y}\cos\theta = 0$$

and

$$\dot{x}\sin(\theta+\phi) - \dot{y}\cos(\theta+\phi) - l\dot{\theta}\cos\phi = 0.$$

Since the rear wheel cannot slide along its rolling direction,

$$\dot{x}\cos\theta + \dot{y}\sin\theta - \rho\dot{\psi} = 0.$$

We may combine the constraint equations in control system form

$$\begin{bmatrix} \dot{x} \\ \dot{y} \\ \dot{\theta} \end{bmatrix} = \begin{bmatrix} \rho\cos\theta \\ \rho\sin\theta \\ (\rho/l)\tan\phi \end{bmatrix} u,$$

where $u = \dot{\psi}$. This equation determines a connection on a trivial principle fiber bundle over M with structure group $G = SE(2)$.

We decompose the arbitrary velocity vector $v_q \in T_qQ$ thus:

$$v_q = \begin{bmatrix} \dot{\phi} \\ \dot{\psi} \\ \dot{x} \\ \dot{y} \\ \dot{\theta} \end{bmatrix} = \begin{bmatrix} \dot{\phi} \\ \dot{\psi} \\ \rho\cos\theta\dot{\psi} \\ \rho\sin\theta\dot{\psi} \\ (\rho/l)\tan\phi\dot{\psi} \end{bmatrix} + \begin{bmatrix} 0 \\ 0 \\ \dot{x} - \rho\cos\theta\dot{\psi} \\ \dot{y} - \rho\sin\theta\dot{\psi} \\ \dot{\theta} - (\rho/l)\tan\phi\dot{\psi} \end{bmatrix} = \mathrm{hor}(v_q) + \mathrm{ver}(v_q).$$

The component $\mathrm{hor}(v_q)$ satisfies the constraints. The vector $\mathrm{ver}(v_q)$ has no base component, and is thus vertical. Since

$$(\Gamma(v_q))_Q(q) = \mathrm{ver}(v_q) = \begin{bmatrix} 0 \\ 0 \\ \dot{x} - \rho\cos\theta\dot{\psi} \\ \dot{y} - \rho\sin\theta\dot{\psi} \\ \dot{\theta} - (\rho/l)\tan\phi\dot{\psi} \end{bmatrix},$$

the connection one-form Γ is given by

$$\Gamma(v_q) = \begin{bmatrix} \dot{x} - (\rho\cos\theta + (\rho/l)y\tan\phi)\dot{\psi} + y\dot{\theta} \\ \dot{y} + ((\rho/l)x\tan\phi - \rho\sin\theta)\dot{\psi} - x\dot{\theta} \\ \dot{\theta} - (\rho/l)\tan\phi\dot{\psi} \end{bmatrix},$$

or

$$\begin{aligned}\Gamma(\dot{r},\dot{g}) &= \begin{bmatrix}\cos\theta & -\sin\theta & y\\ \sin\theta & \cos\theta & -x\\ 0 & 0 & 1\end{bmatrix}\begin{bmatrix}\cos\theta\dot{x}+\sin\theta\dot{y}-\rho\dot{\psi}\\ \cos\theta\dot{y}-\sin\theta\dot{x}\\ \dot{\theta}-(\rho/l)\tan\phi\dot{\psi}\end{bmatrix}\\ &= \begin{bmatrix}\cos\theta & -\sin\theta & y\\ \sin\theta & \cos\theta & -x\\ 0 & 0 & 1\end{bmatrix}\left(\begin{bmatrix}\cos\theta\dot{x}+\sin\theta\dot{y}\\ \cos\theta\dot{y}-\sin\theta\dot{x}\\ \dot{\theta}\end{bmatrix}+\begin{bmatrix}0 & -\rho\\ 0 & 0\\ 0 & -(\rho/l)\tan\phi\end{bmatrix}\begin{bmatrix}\dot{\phi}\\ \dot{\psi}\end{bmatrix}\right)\\ &= \mathrm{Ad}_g(\xi + A(r)\cdot\dot{r}).\end{aligned}$$

Thus

$$A(r) = \begin{bmatrix}-\rho d\psi\\ 0\\ -(\rho/l)\tan\phi d\psi\end{bmatrix}.$$

Since $SE(2)$ is not an Abelian group, the area rule described in Section 4.2 does not apply to this example. It is still possible, however, to generate familiar gaits. Suppose the car is driven back and forth once while the steering wheel is rotated back and forth twice. The resulting figure eight in shape space corresponds to a parallel parking manuever, as shown in [21]. We note that simply driving forward corresponds to a non-simple gait associated with a circle in the ψ variable.

We conclude this example by proving the system's strong controllability. The curvature form is given by

$$\begin{aligned}D\Gamma &= \begin{bmatrix}-(\rho/l)y\sec^2\phi\\ (\rho/l)x\sec^2\phi\\ -(\rho/l)\sec^2\phi\end{bmatrix} d\phi\wedge d\psi\\ &= \begin{bmatrix}\cos\theta & -\sin\theta & y\\ \sin\theta & \cos\theta - x & \\ 0 & 0 & 1\end{bmatrix}\begin{bmatrix}0\\ 0\\ -(\rho/l)\sec^2\phi\end{bmatrix} d\phi\wedge d\psi\\ &= \mathrm{Ad}_g\begin{bmatrix}0\\ 0\\ -(\rho/l)\sec^2\phi d\phi\wedge d\psi\end{bmatrix}\\ &= \mathrm{Ad}_g\, DA(x).\end{aligned}$$

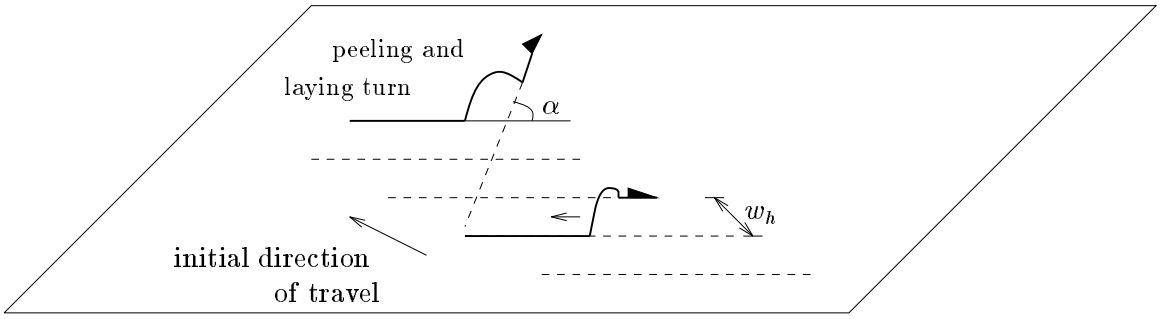

FIGURE 12. Sidewinding motion of a snake.

We compute

$$\{A(X) : X \in TM\} = \mathfrak{h}_1 = \text{span}\begin{bmatrix} \rho \\ 0 \\ (\rho/l)\tan\phi \end{bmatrix},$$

$$\{DA(X,Y) : X, Y \in TM\} = \mathfrak{h}_2 = \text{span}\begin{bmatrix} 0 \\ 0 \\ (\rho/l)\sec^2\phi \end{bmatrix},$$

$$\{L_X DA - [A(X), DA], [DA, DA]\} = \mathfrak{h}_3 = \text{span}\left(\begin{bmatrix} 0 \\ (\rho^2/l)\sec^2\phi \\ 0 \end{bmatrix}, \begin{bmatrix} 0 \\ 0 \\ 2(\rho/l)\sec^2\phi\tan\phi \end{bmatrix}\right),$$

and

$$\mathfrak{h}_4 = \text{span}\left(\begin{bmatrix} 0 \\ 0 \\ 2(\rho/l)(\sec^4\phi + 2\sec^2\phi\tan\phi) \end{bmatrix}, \begin{bmatrix} 0 \\ 2(\rho^2/l)\sec^2\phi\tan\phi \\ 0 \end{bmatrix}, \begin{bmatrix} (\rho^3/l^2)\sec^4\phi \\ 0 \\ 0 \end{bmatrix}\right);$$

the system is locally strongly controllable because $\mathfrak{h}_4$ contains three linearly independent vectors away from $\phi = \pi/2$.

5.2. Sidewinding motion of a snake. We return to the snakelike robot introduced in Section 3.3, and expand our model to encompass locomotion in the plane. The details of the expanded model are presented in Appendix B; the computations and discussion in this section will presume a particular gait.

The system is depicted in Figure 12; we introduce the variable w_h to denote the widthwise span of the hump and α to denote its turning angle. Based on an observation about the nature of sidewinding in real snakes, we assume that the robot comes into contact with the plane only along body segments which remain straight. The internal configuration of the robot is specified by the vector $(l_r, s_h, l_h, w_h, \alpha)$ and its total state by the vector $(l_r, s_h, l_h, w_h, \alpha, x, y, \theta)$. We assume the robot to be sufficiently actuated to control the base variables smoothly while maintaining straight segments of contact.

As before, we assume viscous drag where the robot comes in contact with the ground. Since the sidewinding gait, like the caterpillar gait, is based on the "peeling"

and "laying" of body segments, the choice of friction model is not crucial. Only segments of zero length are dragged along the ground. Our choice allows us to apply our method; the results we obtain will be correct in any case.

We obtain the connection one form from the assumption that the robot must experience zero net viscous drag and moment at all times. Once we have expressions for the net forces in the x and y directions and the net moment about the robot's forward tip, we can solve for $\dot{x}$, $\dot{y}$, and $\dot{\theta}$ in terms of the configuration variables and the remaining velocities. From the decomposition of the system's velocity into horizontal and vertical parts, we proceed as in the previous example to obtain a local connection

$$A(x) = \frac{1}{\Delta}\begin{bmatrix} A_1^{l_r} + A_1^{s_h} + A_1^{l_h} + A_1^{w_h} + A_1^{\alpha} \\ A_2^{l_r} + A_2^{s_h} + A_2^{l_h} + A_2^{w_h} + A_2^{\alpha} \\ A_3^{l_r} + A_3^{s_h} + A_3^{l_h} + A_3^{w_h} + A_3^{\alpha} \end{bmatrix}.$$

As shown in Appendix B, the denominator Δ and the superscripted quantities are given in terms of the shape variables alone.

Since $SE(2)$ is not Abelian, the area rule is not generically applicable to this system. If we are only interested in unidirectional sidewinding, however, we may simplify our model further by assuming that the angles α and θ remain constant, with $\alpha = 0$. The robot will do nothing to turn itself in the plane. We may then assume without loss of generality that $\theta = 0$, and describe the system in terms of a connection on the bundle with Abelian structure group $(\mathbb{R}^2, +)$. The local connection is given by

$$A = \begin{bmatrix} \frac{1-l_r-s_h}{1-s_h}(dl_h - ds_h) \\ \frac{1-l_r-s_h}{1-s_h} dw_h \end{bmatrix}; \tag{42}$$

note the similarity of this expression to that obtained in one dimension. The curvature of this connection is

$$DA = \begin{bmatrix} \frac{1}{1-s_h}(-dl_r \wedge dl_h + dl_r \wedge ds_h + \frac{l_r}{1-s_h} dl_h \wedge ds_h) \\ \frac{1}{1-s_h}(-dl_r \wedge dw_h + \frac{l_r}{1-s_h} dw_h \wedge ds_h) \end{bmatrix}. \tag{43}$$

Since

$$DA \cdot \left(\begin{bmatrix} 0 \\ 1 \\ 0 \\ 0 \end{bmatrix}, \begin{bmatrix} 1 \\ 0 \\ 0 \\ 0 \end{bmatrix} \right) = \begin{bmatrix} 1/(1-s_h) \\ 0 \end{bmatrix}$$

and

$$D\Gamma(l_r, l_h, w_h, s_h) \cdot \left(\begin{bmatrix} 0 \\ 0 \\ 1 \\ 0 \end{bmatrix}, \begin{bmatrix} 1 \\ 0 \\ 0 \\ 0 \end{bmatrix} \right) = \begin{bmatrix} 0 \\ 1/(1-s_h) \end{bmatrix}$$

are linearly independent for $s_h \neq 1$, the system with structure group $(\mathbb{R}^2, +)$ is locally strongly controllable. If the robot executes the cyclic change in shape shown in Figure 13, the x-component of the associated holonomy is

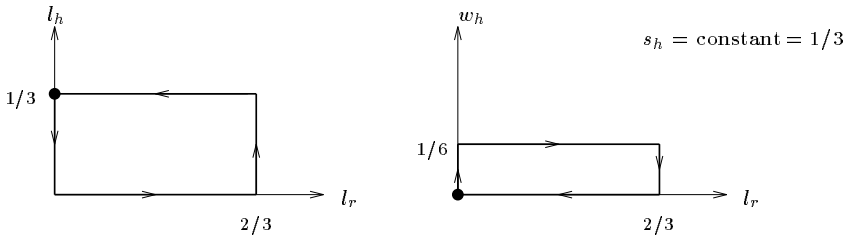

FIGURE 13. Sidewinding gait

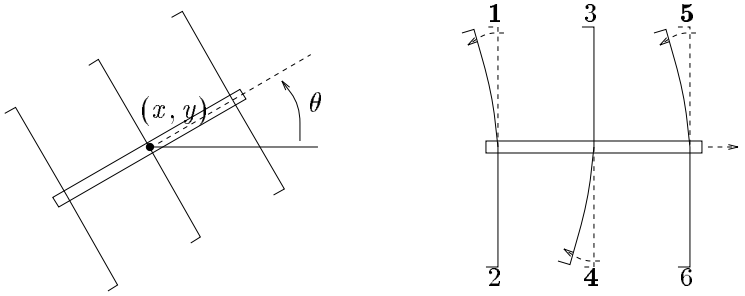

FIGURE 14. A simple six-legged insect robot

$$x(1) = \exp\left(-\iint_S \frac{1}{1-s_h}\, dl_h \wedge dl_r\right)$$
$$= \exp\left(\int_0^{1/3}\int_0^{2/3} \frac{3}{2}\, dl_r dl_h\right) = \exp(1/3) = 1/3$$

and the y-component

$$y(1) = \exp\left(-\iint_S \frac{1}{1-s_h}\, dw_h \wedge dl_r\right)$$
$$= \exp\left(\int_0^{1/6}\int_0^{2/3} \frac{3}{2}\, dl_r dw_h\right) = \exp(1/6) = 1/6.$$

Since the group action is just addition in the group variables, the components of this vector are exactly the net displacements of the system in the x and y directions.

We remark that we can modify this model to allow for multiple humps in the robot's shape and still obtain a connection on a trivial $SE(2)$ bundle. An accurate model for the sidewinding of a real snake would incorporate this change (see [4]).

It is not unique to this problem that we may simplify the relevant geometry with a gait-related assumption; the following model for legged locomotion hinges upon restriction to a particular family of gaits.

5.3. Tripod gait in a six legged robot. Consider the six legged robot shown in Figure 14. Assume that the robot walks with a tripod gait, alternating movements

of legs 1–4–5 with movements of legs 2–3–6. We will suppose that

$$\dot{x} = \cos\theta\Big(\alpha(h_1,h_2)u_1 + \beta(h_1,h_2)u_2\Big)$$

$$\dot{y} = \sin\theta\Big(\alpha(h_1,h_2)u_1 + \beta(h_1,h_2)u_2\Big)$$

$$\dot{\theta} = l\alpha(h_1,h_2)u_1 - l\beta(h_1,h_2)u_2$$

$$\dot{\phi}_1 = u_1 \qquad \dot{h}_1 = v_1$$

$$\dot{\phi}_2 = u_2 \qquad \dot{h}_2 = v_2$$

where

(x, y, θ)	planar position and orientation of the center of mass
ϕ_i	angle of legs, $\phi_i \in [0, \epsilon]$
h_i	height of legs, $h_i \in [0, 1]$.

The variable h_1 denotes the height of legs 1–4–5 and the variable h_2 the height of legs 2–3–6. A height of 1 indicates that a leg is in contact with the ground, while a height of 0 indicates that the leg is raised free. The angles ϕ_i describe the horizontal positions of the legs. The functions α and β relate the propulsive effects of horizontal leg motions to leg height. If the models for the left and right legs are the same, then

$$\beta(h_1,h_2) = \alpha(h_2,h_1).$$

The robot walks forward by lifting and moving the legs with the proper relative phase.

We need a function α which approximately models the following heuristic rules:

(1) If $h_1 = 0$ (no contact) then $\alpha(h_1,h_2) = 0$, indicating that u_1 has no effect on the position of the robot.
(2) If $h_1 = h_2 = 1$ then no net motion should occur since all feet are on the ground.

We select the function

$$\alpha(h_1,h_2) = \begin{cases} |(h_1 - h_2)|^k & h_1 > h_2 \\ 0 & 0 \le h_1 \le h_2 \le 1. \end{cases} \tag{44}$$

This function is C^{k-1} differentiable and has the desired properties. A plot of α for $k = 2$ is shown in Figure 15.

A number of implicit assumptions limit this model's accuracy. We assume, first of all, that the feet do not slip on the ground. Rather than introduce additional degrees of freedom, we model only the effects of the two middle legs, and assume the remaining four to adapt to the no-slip constraint. We also assume that $\phi_i \ll 1$, so that the arcs described by the legs may be treated as straight segments. We have verified through simulations that the model nonetheless captures the basic characteristics of the tripod gait.

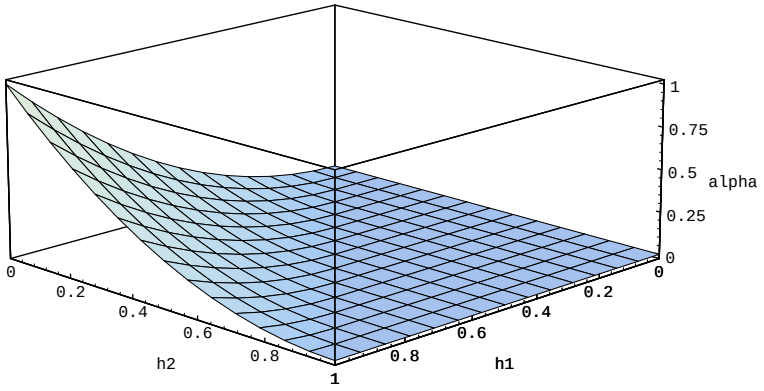

FIGURE 15. Contact function $\alpha(h_1, h_2)$ which models the effect of a given contact as a function of leg heights.

This model defines a connection on $Q = \mathbb{R}^2 \times S^1 \times S^1 \times SE(2)$ with $G = SE(2)$ with local connection one form

$$A(x) = \begin{bmatrix} -\alpha(h_1,h_2)d\phi_1 - \beta(h_1,h_2)d\phi_2 \\ 0 \\ -l\alpha(h_1,h_2)d\phi_1 + l\beta(h_1,h_2)d\phi_2 \end{bmatrix}.$$

Note that although this connection is well-defined for all h_i between 0 and 1, it provides an accurate model of the system only along the boundary of this domain. We only consider gaits for which the connection accurately models the interaction of the robot with its environment.

The computation of the controllability is complicated by the possibly nonsmooth nature of the connection coefficients and the global nature of the paths which interest us. The curvature of the connection has the form

$$DA = \begin{bmatrix} -d\alpha \wedge d\phi_1 - d\beta \wedge d\phi_2 \\ 0 \\ -ld\alpha \wedge d\phi_1 + ld\beta \wedge d\phi_2 \end{bmatrix} + \begin{bmatrix} 0 \\ 2l\alpha\beta d\phi_1 \wedge d\phi_2 \\ 0 \end{bmatrix},$$

where the last term is due to the Lie bracket on $se(2)$. The product $\alpha\beta$ is always zero, however, so only the first term contributes to the system's controllability.

Setting $k = 1$ in equation (44), the curvature of the connection is given for $0 = h_2 < h_1 \leq 1$ by

$$DA(q_1) = \begin{bmatrix} (dh_2 - dh_1) \wedge d\phi_1 \\ 0 \\ l(dh_2 - dh_1) \wedge d\phi_1 \end{bmatrix},$$

and for $0 = h_1 < h_2 \leq 1$ by

$$DA(q_2) = \begin{bmatrix} (dh_1 - dh_2) \wedge d\phi_2 \\ 0 \\ l(dh_2 - dh_1) \wedge d\phi_2 \end{bmatrix}.$$

Since we control h_1 and h_2 directly, we evalute both of these at every reachable point, and observe that the system can move in the direction given by their bracket

$$[DA(q_1), DA(q_2)](X_1, X_2, X_3, X_4) = \begin{bmatrix} 0 \\ 2l\omega_1(X_1, X_2)\omega_2(X_3, X_4) \\ 0 \end{bmatrix},$$

where $\omega_1 = (dh_2 - dh_1) \wedge d\phi_1$ and $\omega_2 = (dh_2 - dh_1) \wedge d\phi_2$. Taking the span of the above forms over vector fields X_i in the base, we conclude that the system can move in any direction in $se(2)$.

An example of the tripod gait is shown in Figure 16. We see that lifting and actuating the two sets of legs in the proper phase generates motion in the x direction. To move in another direction, the robot may change the frequency and phase relationships between the base variables, or move only one set of legs.

Other gait classes may be investigated within this framework, such as that corresponding to pairwise motion of the legs. We could again specify properties of the connection along certain boundaries of shape space according to physical assumption, and choose an appropriately extended connection form.

6. Summary

We have presented the notion of a connection on a principal fiber bundle and demonstrated the modeling of mechanical systems using connections. Connections can represent nonholonomic velocity constraints or conservation laws, and can be used in approximate models for systems with neither of these features. Modeling a system in terms of a connection on a principal bundle simplifies the computations needed to establish its controllability. The splitting of a system's configuration space into base and fiber components further provides a setting for the classification of gaits.

It was our goal to introduce a geometric context within which to study locomotion problems. We have left several issues open. As with any physical theory, ours is useful in a limited variety of situations. Indeed, we have restricted the discussion in this paper to that of systems with constraints of a kinematic nature. The integration of dynamic and kinematic constraints within the framework of connections on bundles is discussed in [2]. We have presented examples which represent the realm of our theory, but we have described no concrete means for recognizing problems which conceal the structure we exploit.

It has been our assumption throughout that a locomotion system has complete control of its own shape. Situations may certainly arise in which a nontrivial control system on the base space of a principal bundle is of interest. We have not explored the interaction of connections with the dynamics of such systems.

It is often the case that the shape space of a robotic system is itself a Lie group. We have made no effort to incorporate this structure into our characterizations of controllability. In [13], Krishnaprasad and Tsakiris examine kinematic chains with nonholonomic constraints which determine connections on principal G-bundles over manifolds of the form $G \times \cdots \times G$.

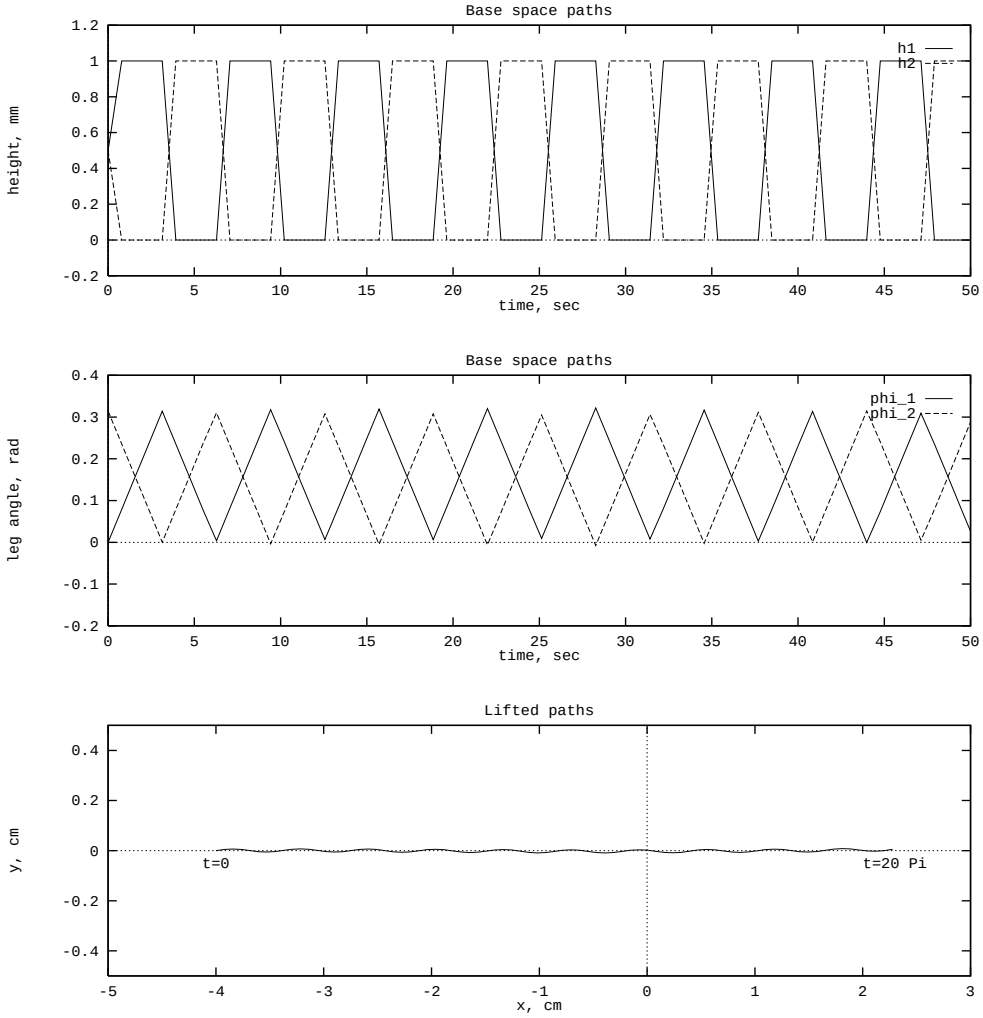

FIGURE 16. Tripod gate for six legged robot. The upper plot shows the motion of the base variables (as a function of time); the lower plot shows the xy motion of the robot (the y scale is enlarged to show the rocking motion).

The algorithm presented in Section 4 for trajectory generation does not guarantee optimal paths. Shapere and Wilczek obtained optimal swimming strokes for paramecia in [26], and Montgomery discusses the general problem of optimal control on principal bundles in [18].

We have spoken only briefly of the classification of gaits in terms of their representations in base space. In pursuing this notion, we may gain insight from classifying systems themselves according to the classes of gaits needed to control them. Only some systems, for instance, require the Lie bracketing of control vectors to exhibit weak controllabilty.

We have approached the modeling of snakelike robots in search of finite dimensional parametrizations of shape space. In [27], Shapere and Wilczek developed an infinite dimensional description of a self-propelling paramecium, resorting to a finite approximation for computational purposes only. Our approach was simpler for us; it is not clear if either approach to modeling infinite dimensional systems is better in general. An infinite dimensional model may represent a more rigorous description of a system's behavior, but we have not considered the subtleties of principal bundles over infinite dimensional spaces.

We have examined existing results in the geometric mechanics of systems on principal bundles through a control theoretic lens. In graduating to problems which involve dynamic, as well as kinematic, constraints, we enter the realm of control systems with drift. In the future we hope to extend our discussion beyond that of driftless systems.

Acknowledgements. The authors would like to thank Joel Burdick and Andrew Lewis for their collaborative efforts on this work. Their input and feedback is very much appreciated. We would also like to thank Jair Koiller, Richard Montgomery, and Jerry Marsden for their insight and encouragement. Scott Kelly's research is supported in part by an ONR Graduate Fellowship.

References

1. D. Bleeker. *Gauge Theory and Variational Principles.* Addison-Wesley, 1981.
2. A. M. Bloch, P. S. Krishnaprasad, J. E. Marsden, and R. M. Murray. Nonholonomic mechanical systems with symmetry. Work in progress.
3. W. M. Boothby. *An Introduction to Differentiable Manifolds and Riemannian Geometry.* Academic Press, second edition, 1986.
4. J. W. Burdick, J. Radford, and G. S. Chirikjian. The Kinematics of Hyper-Redundant Locomotion. *Advanced Robotics*, 1994 (to appear).
5. G. S. Chirikjian and J. W. Burdick. The Kinematics of Hyper-Redundant Locomotion. *IEEE Trans. on Robotics and Automation*, 1994 (to appear).
6. Sir James Gray. *Animal Locomotion.* Weidenfeld & Nicolson, 1968.
7. M. Hildebrand. Symmetrical gaits of horses. *Science*, 150: 701-709, 1967.
8. S. Hirose and Y. Umetani. Kinematic control of an active cord mechanism with tactile sensors. *2nd CISM-IFToMM Symp. on Theory & practice of Robots & Manipulators*, Elsevier, 1977 [1976], pp. 241–252.
9. S. Hirose, Y. Umetani, S. Oda. An active cord mechanism with oblique swivel joints, and its control. *4th CISM-IFToMM Symp. on Theory & practice of Robots & Manipulators* PWN, Warsaw, 1983 [1981], pp. 327 –340.
10. A. C. Hutchinson. Machines can walk. *The Chartered Mechanical Engineer*, November 1967.
11. J. B. Keller and M. S. Falkovitz. Crawling of worms. *Journal of Theoretical Biology*, 104:417–442, 1983.
12. S. Kobayashi and K. Nomizu. *Foundations of Diiferential Geometry, Volume 1*, volume 1. John Wiley and Sons, 1963.
13. P. S. Krishnaprasad and D. P. Tsakiris. G–snakes: nonholonomic kinematic chains on Lie groups. *IEEE Conf. on Decision and Control*, to appear.
14. A. Lewis, J. P. Ostrowski, R. M. Murray, and J. Burdick. Nonholonomic mechanics and locomotion: the snakeboard example. *IEEE Intern. Conf. on Robotics and Automation*, to appear.
15. J. Marsden, R. Montgomery, and T. Ratiu. Reduction, symmetry, and phases in mechanics. *Memoirs of the American Mathematical Society*, 88(436), 1990.
16. T. McGeer. Dynamics and control of bipedal locomotion. *Journal of Theoretical Biology*, 163(3): 277–314, 1993.
17. R. B. McGhee. Some finite state aspects of legged locomotion. *Mathematical Biosciences*, 2(1/2): 67–84, 1968.
18. R. Montgomery. Nonholonomic control and gauge theory. In Z. Li and J. F. Canny, editors, *Nonholonomic Motion Planning*, pages 343–378. Kluwer, 1993.
19. R. S. Mosher. Test and evaluation of a versatile walking truck. *Proceedings of Off-Road Mobility Research Symposium*, International Society for Terrain Vehicle Systems, Washington, D. C.: 359–379, 1968.
20. R. M. Murray, Z. Li, and S. S. Sastry. *A Mathematical Introduction to Robotic Manipulation.* CRC Press, 1994.
21. R. M. Murray and S. S. Sastry. Nonholonomic motion planning: Steering using sinusoids. *IEEE Transactions on Automatic Control*, 38(5):700–716, 1993.
22. E. Muybridge. *The Human Figure in Motion.* Dover Publications, 1955 (first published in 1901).
23. E. Muybridge. *Animals in Motion.* Dover Publications, 1958 (first published in 1899).

24. M. H. Raibert. *Legged Robots That Balance*. MIT Press, 1986.
25. M. H. Raibert and I. E. Sutherland. Machines that walk. *Scientific American*, 248(2): 44–53.
26. A. Shapere and F. Wilczek. Efficiencies of self-propulsion at low Reynolds number. *Journal of Fluid Mechanics*, 198:587–599, 1989.
27. A. Shapere and F. Wilczek. Geometry of self-propulsion at low Reynolds number. *Journal of Fluid Mechanics*, 198:557–585, 1989.
28. R. Tomovic and W. J. Karplus. Land locomotion simulation and control. *Proceedings Third International Analogue Computation Meeting*, Opatija, Yugoslavia, 1961, pp. 385–390.

Appendix A. Proof of Proposition 5

We now demonstrate that the criteria advanced in Proposition 5 for strong and weak controllability are precisely those obtained from Chow's theorem. In order to apply Chow's theorem, we compute the Lie algebra generated by the horizontal lifts X_i^h of vector fields X_i on M. We will show that the fiber components of elements of this Lie algebra may be written in terms of the connection one form, its curvature, and higher order Lie derivatives. In particular, each level of bracketing adds another of the sets $\mathfrak{h}_i$ to the set of fiber directions in which we can steer from a configuration $q = (x, e) \in Q$.

Every bracket calculation will fall into one of three categories. We will begin by obtaining a general expression for brackets of the form $[X_i^h, X_j^h]$. It will become clear that such brackets are, in fact, vertical vector fields. We will then obtain an expression for the bracket between a vertical vector field and one of the X_i^h. These brackets will also turn out to be vertical. We will conclude with an expression for the bracket between two vertical vector fields.

In computing the Lie algebra generated by the X_i^h, we are primarily interested in the fiber components of the vectors we obtain. A system will be weakly controllable if and only if the X_i^h generate a set of vectors whose fiber components span the full space of group velocities. Our notion of strong controllability is controllability in the usual sense. A system will be strongly controllable if and only if the Lie algebra generated by the X_i^h contains sufficiently many linearly independent vectors to span the tangent space T_qQ a point $q \in Q$.

We begin with a few preliminary facts; their proofs, where omitted, can be found in [12].

Lemma 2. *Suppose $Q \to Q/G = M$ is a trivial principal bundle with connection $\Gamma : TQ \to \mathfrak{g}$. If $X, Y \in TM \subset TQ$ then*

$$\mathrm{hor}[X^h, Y^h] = \mathrm{hor}[X, Y] + [X, Y]^h.$$

Lemma 3. *Let $\Phi : G \times Q \to Q$ be an action of G on Q with infinitesimal generator $\xi_Q \in TQ$ for $\xi \in \mathfrak{g}$. If $\xi, \eta \in \mathfrak{g}$ then*

$$[\xi_Q, \eta_Q] = -[\xi, \eta]_Q.$$

Lemma 4. *Let X and Y be vector fields on Q and Γ the connection one form. Then*

$$\begin{aligned}\Gamma([X, Y]) &= X\Gamma(Y) - Y\Gamma(X) - d\Gamma(X, Y) \\ &= X\Gamma(Y) - Y\Gamma(X) - D\Gamma(X, Y) - [\Gamma(X), \Gamma(Y)].\end{aligned}$$

We will often use this formula in conjunction with the fact that Γ evaluates to zero on horizontal vector fields.

Lemma 5. *Let Z and W be vertical vector fields on Q. Then*

$$\Gamma([Z, W]) = -[\Gamma(Z), \Gamma(W)].$$

Proof. By Lemma 3,

$$\begin{aligned}\Gamma([Z,W]) &= \Gamma([\operatorname{ver} Z, \operatorname{ver} W]) = \Gamma([\Gamma_Q(Z), \Gamma_Q(W)]) \\ &= \Gamma(-[\Gamma(Z), \Gamma(W)]_Q) = -[\Gamma(Z), \Gamma(W)].\end{aligned}$$

□

We now recall that any vertical vector field Z on Q may be written as the infinitesimal generator $\Gamma_Q(Z)$. This follows from the definition of the connection one form.

Lemma 6. *If $Z = \Gamma_Q(Z)$ is a vertical vector field on Q, its component $\dot{x}(Z)$ in the base is zero and its fiber component $\dot{g}(Z)$ satisfies*

$$\Gamma(Z) = \operatorname{Ad}_g g^{-1}\dot{g}(Z) = \dot{g}(Z)g^{-1},$$

or

$$\dot{g}(Z) = g \operatorname{Ad}_g^{-1} \Gamma(Z) = \Gamma(Z)g.$$

Proof. This follows from equation (15) of Section 2.3. □

***Proof of Proposition* 5.** We are finally ready for the proof. We begin with a choice of m linearly independent vector fields $X_1 \ldots X_m$ on M, where m is equal to the dimension of M. We may assume, without loss of generality, that $[X_i, X_j] = 0$ for all i, j. This is true, for instance, when $X_i = \frac{\partial}{\partial x_i}$, as in equation (28) of Section 4. The group velocities corresponding to the vectors X_i^h are given by

$$\dot{g}(X_i^h) = -gA(X_i). \tag{45}$$

This follows from equation (15) and the fact that $\Gamma(X_i^h) = 0$.

We compute the first set of Lie brackets. By Lemma 2,

$$\operatorname{hor}[X_i^h, X_j^h] = [X_i, X_j]^h = 0;$$

thus $[X_i^h, X_j^h]$ is vertical. By Lemma 6, then,

$$\dot{g}([X_i^h, X_j^h]) = g \operatorname{Ad}_g^{-1} \Gamma([X^h, Y^h]).$$

By Lemma 4, however,

$$\begin{aligned}\Gamma([X_i^h, X_j^h]) &= L_{X_i^h}\Gamma(X_j^h) - L_{X_j^h}\Gamma(X_i^h) - D\Gamma(X_i^h, X_j^h) - [\Gamma(X_i^h), \Gamma(X_j^h)] \\ &= -D\Gamma(X_i^h, X_j^h) \\ &= -\operatorname{Ad}_g DA(X_i, X_j),\end{aligned}$$

so

$$\dot{g}([X_i^h, X_j^h]) = -g \operatorname{Ad}_g^{-1} \operatorname{Ad}_g DA(X_i, X_j) = -gDA(X_i, X_j). \tag{46}$$

So far, we have determined the fiber components of the vectors generated by the X_i^h through one level of bracketing. Let us next consider brackets of the form $[[X_i^h, X_j^h], X_k^h]$. The base component of $[X_i^h, X_j^h]$ is zero and that of X_k^h is simply

X_k. Since X_k is a vector field on M, $[[X_i^h, X_j^h], X_k^h]$ is vertical. It follows from equations (45) and (46) that

$$\begin{aligned}\dot{g}([[X_i^h, X_j^h], X_k^h]) &= -L_{X_k}(-gDA(X_i, X_j)) + [gDA(X_i, X_j), gA(X_k)] \\ &= -g\left(L_{X_k}DA(X_i, X_j) - [A(X_k), DA(X_i, X_j)]\right).\end{aligned}$$

It should be clear at this point that any remaining elements of the Lie algebra generated by the X_i can be written as (possibly compound) brackets of those we have obtained thus far. We have, in particular, obtained expressions for the fiber components $\dot{g}(\cdot)$ of each of the vectors we have considered. Let us now assume Z to be any vertical vector field on Q, with group velocity $\dot{g}(Z)$. It is straightforward to show that $\dot{x}([X_i^h, Z]) = 0$, and that

$$\dot{g}([X_i^h, Z]) = L_{X_i}\dot{g}(Z) - [gA(X_i), \dot{g}(Z)]. \tag{47}$$

If Z and W are both vertical vector fields, Lemmas 5 and 6 imply that the fiber component of $[Z, W]$ satisfies

$$\begin{aligned}\dot{g}([Z, W]) &= \Gamma([Z, W])g = -[\Gamma(Z), \Gamma(W)]g \\ &= -[\dot{g}(Z)g^{-1}, \dot{g}(W)g^{-1}]g = -[\dot{g}(Z), \dot{g}(W)]g^{-1}g \\ &= -[\dot{g}(Z), \dot{g}(W)].\end{aligned} \tag{48}$$

We have obtained expressions for the fiber components of all elements of the Lie algebra generated by the vector fields X_i^h. Our tests for strong and weak controllability will ask that certain subsets of these span the space of all group velocities. Before we specify these, however, we may exploit the arbitrary nature of our choice of group element g to simplify matters further. Since the kinematics of a system modeled on a principal bundle $Q = M \times G$ are independent of its position and orientation, we need only examine the controllability of such a system at points in Q corresponding to $g = e$. If the system is (strongly or weakly) controllable at a particular point q in the fiber over $x \in M$, it will be controllable at all points along that fiber.

The assumption that $g = e$ permits us not only to simplify the expressions we have obtained for the group velocities $\dot{g}(\cdot)$, but also to equate these velocities with Lie algebra elements. Equation (45) becomes

$$\dot{g}(X_i^h) = -A(X_i), \tag{49}$$

equation (46) becomes

$$\dot{g}(X_i^h, X_j^h) = -DA(X_i, X_j), \tag{50}$$

equation (47) becomes

$$\dot{g}([X_i^h, Z]) = L_{X_i}\dot{g}(Z) - [A(X_i), \dot{g}(Z)], \tag{51}$$

and equation (48) remains

$$\dot{g} = -[\dot{g}(Z), \dot{g}(W)]. \tag{52}$$

We will now formulate the criterion for weak controllability. The space of group velocities at any configuration $q = (x, e)$ is exactly the Lie algebra $\mathfrak{g}$ of the structure group G. A system will be weakly controllable, then, if and only if the fiber components of the Lie algebra generated by the vector fields X_i^h at $q = (x, g)$ span the Lie algebra $\mathfrak{g}$. Before any bracketing, the vector fields X_i^h provide us with the fiber velocities $A(X_i)$, as shown by equation (49). Note that the span of these Lie algebra elements is precisely the set $\mathfrak{h}_1$ defined in Section 4. After one level of bracketing, we obtain the additional fiber velocities spanned by $DA(X_i, X_j)$, as shown by equation (50). These constitute the set $\mathfrak{h}_2$. Proceeding with equations (51) and (52), we observe that each level of bracketing augments the set of available group velocities with one of the $\mathfrak{h}_i$. It follows that a system is locally weakly controllable if and only if

$$\mathfrak{g} = \mathfrak{h}_1 \oplus \mathfrak{h}_2 \oplus \mathfrak{h}_3 \oplus \cdots .$$

Let us now address strong controllability. By Chow's theorem, a system is strongly controllable near a point $q = (r, e)$ if and only if the Lie algebra generated by the vector fields X_i^h spans $\mathfrak{g}$ at that point. We have chosen the vector fields $X_1, \ldots, X_m$ on M such that $X_1^h, \ldots, X_m^h$ are linearly independent. Recall that all elements of the Lie algebra generated by the X_i^h which were not contained in their span were vertical. Since no vertical vector field can lie in the span of the horizontal vector fields X_i^h, the system will be strongly controllable if and only if the Lie algebra generated by the X_i^h contains $n - m$ linearly independent vertical vector fields. Since the base velocity corresponding to any vertical vector is zero, this will be the case if and only if the X_i^h generate $n - m$ vertical vector fields with linearly independent fiber components. The fiber components of the vertical vector fields generated by the X_i^h are given collectively by $\mathfrak{h}_2 \oplus \mathfrak{h}_3 \oplus \cdots$. Since the dimension of the structure group G is equal to $n - m$, the system will be locally strongly controllable near $q = (r, e)$ if and only if

$$\mathfrak{g} = \mathfrak{h}_2 \oplus \mathfrak{h}_3 \oplus \cdots .$$

□

Appendix B. Derivation of connection form for sidewinder

We now derive the connection one form for the snakelike robot of Section 5.2. The robot will experience zero net drag provided

$$0 = F_1^{l_r} + F_1^{s_h} + F_1^{l_h} + F_1^{w_h} + F_1^{\alpha} + F_1^{x} + F_1^{y} + F_1^{\theta}$$

and

$$0 = F_2^{l_r} + F_2^{s_h} + F_2^{l_h} + F_2^{w_h} + F_2^{\alpha} + F_2^{x} + F_2^{y} + F_2^{\theta},$$

where

$$\begin{aligned}
F_1^{l_r} &= 2(1 - l_r - s_h)\sin\frac{\alpha}{2}\sin(\frac{\alpha}{2} + \theta);\\
F_1^{s_h} &= (-1 + l_r + s_h)\cos(\alpha + \theta);\\
F_1^{l_h} &= (1 - l_r - s_h)\cos\theta;\\
F_1^{w_h} &= (-1 + l_r + s_h)\sin\theta;\\
F_1^{\alpha} &= \frac{-1}{2}((-1 + l_r + s_h)^2\sin(\alpha + \theta));\\
F_1^{x} &= 1 - s_h;\\
F_1^{y} &= 0;\\
F_1^{\theta} &= (-1 + l_r + s_h)w_h\cos\theta + (-l_h - l_r + l_h l_r + l_r^2/2 + l_h s_h + l_r s_h)\sin\theta\\
&\quad - \frac{1}{2}((-1 + l_r + s_h)^2\sin(\alpha + \theta))
\end{aligned}$$

and

$$\begin{aligned}
F_2^{l_r} &= 2(-1 + l_r + s_h)\cos(\frac{\alpha}{2} + \theta)\sin\frac{\alpha}{2};\\
F_2^{s_h} &= (-1 + l_r + s_h)\sin(\alpha + \theta);\\
F_2^{l_h} &= (1 - l_r - s_h)\sin\theta;\\
F_2^{w_h} &= (1 - l_r - s_h)\cos\theta;\\
F_2^{\alpha} &= \frac{1}{2}((-1 + l_r + s_h)^2\cos(\alpha + \theta));\\
F_2^{x} &= 0;\\
F_2^{y} &= 1 - s_h;\\
F_2^{\theta} &= (l_h + l_r - l_h l_r - l_r^2/2 - l_h s_h - l_r s_h)\cos\theta + \frac{1}{2}((-1 + l_r + s_h)^2\cos(\alpha + \theta))\\
&\quad - (1 + l_r + s_h)w_h\sin\theta.
\end{aligned}$$

The net moment about the robot's forward tip must also remain zero at all times; thus

$$0 = M^{l_r} + M^{s_h} + M^{l_h} + M^{w_h} + M^{\alpha} + M^{x} + M^{y} + M^{\theta},$$

where

$$
\begin{aligned}
M^{l_r} &= (-1+l_r+s_h)\sin\frac{\alpha}{2}((1+2l_h+l_r-s_h)\cos\frac{\alpha}{2}+2w_h\sin\frac{\alpha}{2});\\
M^{s_h} &= (-1+l_r+s_h)(-(w_h\cos\alpha)+(l_h+l_r)\sin\alpha);\\
M^{l_h} &= \frac{1}{2}((-1+l_r+s_h)(2w_h+(1-l_r-s_h)\sin\alpha));\\
M^{w_h} &= \frac{1}{2}((-1+l_r+s_h)(-2l_h-2l_r+(-1+l_r+s_h)\cos\alpha));\\
M^{\alpha} &= \frac{1}{6}((-1+l_r+s_h)^2(2-2l_r-2s_h+3(l_h+l_r)\cos\alpha+3w_h\sin\alpha));\\
M^{x} &= (-1+l_r+s_h)w_h\cos\theta+(1-l_h-l_r+l_hl_r+l_r^2/2+l_hs_h+l_rs_h)\sin\theta\\
&\quad+(\frac{1}{2}+l_r-\frac{l_r^2}{2}+s_h-l_rs_h-\frac{s_h^2}{2})\sin(\alpha+\theta);\\
M^{y} &= (l_h+l_r-l_hl_r-\frac{l_r^2}{2}-l_hs_h-l_rs_h)\cos\theta+\frac{1}{2}((-1+l_r+s_h)^2\cos(\alpha+\theta))\\
&\quad+(1-w_h+l_rw_h+s_hw_h)\sin\theta;\\
M^{\theta} &= \frac{1}{3}+l_h^2-l_r+2l_hl_r-l_h^2l_r+2l_r^2-2l_hl_r^2-l_r^3-s_h-l_h^2s_h+2l_rs_h-2l_hl_rs_h-2l_r^2s_h+s_h^2\\
&\quad-l_rs_h^2-\frac{s_h^3}{3}+w_h^2-l_rw_h^2-s_hw_h^2+(l_h+l_r)(-1+l_r+s_h)^2\cos\alpha+(-1+l_r+s_h)^2w_h\sin\alpha.
\end{aligned}
$$

These constraints define the local connection

$$
A(x)=\frac{1}{\Delta}\begin{bmatrix}A_1^{l_r}+A_1^{s_h}+A_1^{l_h}+A_1^{w_h}+A_1^{\alpha}\\ A_2^{l_r}+A_2^{s_h}+A_2^{l_h}+A_2^{w_h}+A_2^{\alpha}\\ A_3^{l_r}+A_3^{s_h}+A_3^{l_h}+A_3^{w_h}+A_3^{\alpha}\end{bmatrix}
$$

on the trivial principal bundle over $M\subset\mathbb{R}^2\times SE(2)$ with structure group $SE(2)$, where

$$
\begin{aligned}
\Delta &= 2(-1+s_h)(1+12l_h^2l_r-6l_r^2+12l_hl_r^2-12l_h^2l_r^2+12l_r^3-12l_hl_r^3-6l_r^4-4s_h\\
&\quad-12l_h^2l_rs_h+12l_r^2s_h-12l_hl_r^2s_h-12l_r^3s_h+6s_h^2-6l_r^2s_h^2-4s_h^3+s_h^4\\
&\quad+12l_rw_h^2-12l_r^2w_h^2-12l_rs_hw_h^2+6l_r(2l_h+l_r)(-1+l_r+s_h)^2\cos\alpha\\
&\quad+12l_r(-1+l_r+s_h)^2w_h\sin\alpha);
\end{aligned}
$$

$$
\begin{aligned}
A_1^{l_r} &= 2(-1+l_r+s_h)\sin\frac{\alpha}{2}(12l_r(1-l_r-s_h)w_h\cos\frac{\alpha}{2}(-2l_h-l_r-(1+l_r+s_h)\cos\alpha)\\
&+2(1-3l_r-6l_hl_r+12l_h^2l_r+24l_hl_r^2-12l_h^2l_r^2+9l_r^3-18l_hl_r^3-6l_r^4\\
&-4s_h+9l_rs_h+12l_hl_rs_h-12l_h^2l_rs_h-24l_hl_r^2s_h-9l_r^3s_h+6s_h^2-9l_rs_h^2\\
&-6l_hl_rs_h^2-4s_h^3+3l_rs_h^3+s_h^4+3l_r(-1+l_r+s_h)^2(-1+2l_h+2l_r+s_h)\cos\alpha)\sin\frac{\alpha}{2})\\
&-12l_r(-1+l_r+s_h)^2(l_r+s_h)w_h\sin 2\alpha;\\
A_1^{s_h} &= (1-l_r-s_h)(18l_hl_r+9l_r^2-36l_hl_r^2-18l_r^3+18l_hl_r^3+9l_r^4-36l_hl_rs_h\\
&-18l_r^2s_h+36l_hl_r^2s_h+18l_r^3s_h+18l_hl_rs_h^2\\
&+9l_r^2s_h^2+2(1+12l_h^2l_r-6l_r^2+12l_hl_r^2-12l_h^2l_r^2+12l_r^3-12l_hl_r^3\\
&-6l_r^4-4s_h-12l_h^2l_rs_h+12l_r^2s_h-12l_hl_r^2s_h-12l_r^3s_h+6s_h^2-6l_r^2s_h^2\\
&-4s_h^3+s_h^4)\cos\alpha+3l_r(2l_h+l_r)(-1+l_r+s_h)^2\cos 2\alpha\\
&+12l_r(-1+l_r+s_h)w_h(-2l_h-l_r-\cos\alpha+l_r\cos\alpha+s_h\cos\alpha)\sin\alpha);\\
A_1^{l_h} &= (-1+l_r+s_h)(2-3l_r+24l_h^2l_r-3l_r^2+24l_hl_r^2-24l_h^2l_r^2+15l_r^3-24l_hl_r^3\\
&-9l_r^4-8s_h+9l_rs_h-24l_h^2l_rs_h+6l_r^2s_h-24l_hl_r^2s_h-15l_r^3s_h+12s_h^2\\
&-9l_rs_h^2-3l_r^2s_h^2-8s_h^3+3l_rs_h^3+2s_h^4+12l_r(2l_h+l_r)(-1+l_r+s_h)^2\cos\alpha\\
&+3l_r(1-l_r-s_h)^3\cos 2\alpha);\\
A_1^{w_h} &= 6l_r(-1+l_r+s_h)^2(2l_h+l_r+(1-l_r-s_h)\cos\alpha)(-2w_h+(-1+l_r+s_h)\sin\alpha);\\
A_1^{\alpha} &= \frac{1}{2}((-1+l_r+s_h)^2(-4w_h+2l_rw_h+8l_r^2w_h-6l_r^3w_h+12s_hw_h-4l_rs_hw_h\\
&-8l_r^2s_hw_h-12s_h^2w_h+2l_rs_h^2w_h+4s_h^3w_h+6l_r(-1+l_r+s_h)w_h((4l_h+2l_r)\cos\alpha\\
&+(1-l_r-s_h)\cos 2\alpha)+2l_r(12l_h^2+12l_hl_r-12l_h^2l_r+4l_r^2\\
&-12l_hl_r^2-3l_r^3-12l_h^2s_h-12l_hl_rs_h-4l_r^2s_h+3(2l_h+l_r)(-1+l_r+s_h)^2\cos\alpha)\sin\alpha));\\
A_2^{l_r} &= 2(1-l_r-s_h)\sin\frac{\alpha}{2}(2\cos\frac{\alpha}{2}(1-6l_hl_r-12l_r^2+6l_hl_r^2+15l_r^3\\
&-6l_hl_r^3-6l_r^4-4s_h+12l_hl_rs_h+24l_r^2s_h-6l_hl_r^2s_h-15l_r^3s_h+6s_h^2-6l_hl_rs_h^2\\
&-12l_r^2s_h^2-4s_h^3+s_h^4+12l_rw_h^2-12l_r^2w_h^2-12l_rs_hw_h^2+3l_r(-1+l_r+s_h)^2(-1+2l_h\\
&+2l_r+s_h)\cos\alpha)+12l_rw_h(2-2l_h-6l_r+2l_hl_r+3l_r^2-4s_h+2l_hs_h\\
&+6l_rs_h+2s_h^2+(-1+l_r+s_h)^2\cos\alpha)\sin\frac{\alpha}{2});\\
A_2^{s_h} &= (1-l_r-s_h)(18l_rw_h-36l_r^2w_h+18l_r^3w_h-36l_rs_hw_h+36l_r^2s_hw_h+18l_rs_h^2w_h\\
&+6l_rw_h(2(2l_h+2l_r-2l_hl_r-l_r^2-2l_hs_h-2l_rs_h)\cos\alpha-(-1+l_r+s_h)^2\cos 2\alpha)\\
&+2(1-6l_r^2-6l_hl_r^2+6l_r^3-3l_r^4-4s_h+12l_r^2s_h+6l_hl_r^2s_h-6l_r^3s_h+6s_h^2\\
&-6l_r^2s_h^2-4s_h^3+s_h^4+12l_rw_h^2-12l_r^2w_h^2-12l_rs_hw_h^2+3l_r(2l_h+l_r)(-1+l_r+s_h)^2\cos\alpha)\sin\alpha);\\
A_2^{l_h} &= 6l_r(-1+l_r+s_h)(2l_h+2l_r-2l_hl_r-l_r^2-2l_hs_h-2l_rs_h\\
&+(-1+l_r+s_h)^2\cos\alpha)(2w_h+(1-l_r-s_h)\sin\alpha);
\end{aligned}
$$

$$
\begin{aligned}
A_2^{w_h} &= (-1+l_r+s_h)(2-3l_r-3l_r^2-12l_hl_r^2+3l_r^3-3l_r^4-8s_h+9l_rs_h+6l_r^2s_h+12l_hl_r^2s_h\\
&\quad -3l_r^3s_h+12s_h^2-9l_rs_h^2-3l_r^2s_h^2-8s_h^3+3l_rs_h^3+2s_h^4+24l_rw_h^2-24l_r^2w_h^2\\
&\quad -24l_rs_hw_h^2+3l_r(2l_r(1-s_h)(-1+l_r+s_h)\cos\alpha\\
&\quad +(-1+l_r+s_h)^3\cos 2\alpha)+24l_r(-1+l_r+s_h)^2w_h\sin\alpha);\\
A_2^{\alpha} &= \frac{1}{2}((-1+l_r+s_h)^2(4l_h+4l_ry-2l_hl_r+3l_r^2-8l_hl_r^2-10l_r^3+6l_hl_r^3+3l_r^4-12l_hs_h\\
&\quad -12l_rs_h+4l_hl_rs_h-6l_r^2s_h+8l_hl_r^2s_h+10l_r^3s_h+12l_hs_h^2+12l_rs_h^2\\
&\quad -2l_hl_rs_h^2+3l_r^2s_h^2-4l_hs_h^3-4l_rs_h^3+l_r(4(3l_hl_r+l_r^2-3l_hl_rs_h-l_r^2s_h\\
&\quad -6w_h^2+6l_rw_h^2+6s_hw_h^2)\cos\alpha-3(2l_h+l_r)(-1+l_r+s_h)^2\cos 2\alpha)\\
&\quad +12l_rw_h(2l_h+2l_r-2l_hl_r-l_r^2-2l_hs_h-2l_rs_h+(-1-2l_r+l_r^2\\
&\quad -2s_h+2l_rs_h+s_h^2)\cos\alpha)\sin\alpha))\\
&\quad +6l_r(-1+l_r+s_h)^2(2l_r-l_r^2+2s_h-2l_rs_h-s_h^2)w_h\sin 2\alpha;\\
A_3^{l_r} &= 24l_r(-1+s_h)(-1+l_r+s_h)\sin\frac{\alpha}{2}((1+2l_h-s_h)\cos\frac{\alpha}{2}+2w_h\sin\frac{\alpha}{2});\\
A_3^{s_h} &= 12l_r(-1+s_h)(-1+l_r+s_h)(-2w_h\cos\alpha+(2l_h+l_r)\sin\alpha);\\
A_3^{l_h} &= 12l_r(1-s_h)(-1+l_r+s_h)(-2w_h+(-1+l_r+s_h)\sin\alpha);\\
A_3^{w_h} &= 12l_r(-1+s_h)(-1+l_r+s_h)(-2l_h-l_r+(-1+l_r+s_h)\cos\alpha);\\
A_3^{\alpha} &= 2(-1+s_h)(-1+l_r+s_h)^2(1+2l_r-3l_r^2-2s_h-2l_rs_h+s_h^2+3l_r(2l_h+l_r)\cos\alpha+6l_rw_h\sin\alpha).
\end{aligned}
$$